

Supporting Information

API Continuous Cooling and Antisolvent Crystallization for Kinetic Impurity Rejection in cGMP Manufacturing

Martin D. Johnson, Christopher L. Burcham*, Scott A. May, Joel R. Calvin, Jennifer McClary Groh, Steven S Myers, Luke P. Webster, Jeffrey C. Roberts, Venkata Ramana Reddy, Carla V. Luciani*

Eli Lilly and Company, Process Development, Indianapolis, Indiana 46285, USA

Aoife P. Corrigan, Richard D. Spencer, Robert Moylan, Raymond Boyse, John D Murphy

Eli Lilly Kinsale, Manufacturing, Dunderrow, Kinsale, Cork, Ireland

James R. Stout

D&M Continuous Solutions, LLC, Greenwood, IN 46113, USA

*corresponding authors

<johnson_martin_d@lilly.com>; <burcham_christopher_l@lilly.com>

Contents

1. Original batch process.....	3
2. Equipment and automation descriptions	4
2.a. Research scale systems.....	4
2 MSMPRs in series.....	4

3 MSMPRs in series.....	7
2.b. Pilot scale. 250 mL evaporator, three 2 L MSMPRs in series, and dual 250 mL agitated filters	8
2.c. Manufacturing scale continuous distillation in the development lab.....	11
2.d. cGMP manufacturing.....	12
Evaporator	12
3 MSMPRs in series.....	13
Dual slurry-off filtration	15
3. Particle Size Distribution Data	29
4. Exploratory Data Analysis	31
4.a. Research scale PSD	31
4.b. Supersaturation	33
5. Microscopy	36
5.a. Research scale crystallizations.....	36
5.b. Pilot scale crystallizations	45
5.c. Manufacturing scale crystallizations.....	47
6. RTD Model Equations	51
7. Solubility Measurements.....	60
8. Population Balance Model – Scale Dependent.....	61
9. References	65

Table of Figures

Figure S1. Schematic for 2 MSMPRs in series system.....	19
Figure S2. Schematic for 3 MSMPRs in series at research scale.	20
Figure S3. Picture of the 3 MSMPRs in series operating at research scale, MSMPR1, 2 and 3 from left to right.	21
Figure S4. Schematic diagram for the 250 mL evaporator, three 2 L MSMPRs in series, and 80 mm diameter jacketed glass dual slurry-off filters.	22
Figure S5. Picture of the 250 mL continuous evaporator, three 2 L MSMPRs, and one of the dual slurry-off filters while running at steady state.....	23
Figure S6. Foaming after the first 15 min running the evaporator. (a), Evaporator started refluxing with only THF. (b), evaporator started with 95/5 THF/water v/v. (c) evaporator started with representative crude API feed solution.	24
Figure S7. Process diagram for manufacturing scale evaporator tested in development labs.	25
Figure S8. Schematic of the cGMP manufacturing plant evaporator.	26
Figure S9. Schematic of the cGMP manufacturing plant MSMPRs in series.....	27

Figure S10. Schematic of dual filter skid in manufacturing.	28
Figure S11. Filter agitator seals used at the beginning of the campaign. These are the O-rings that shed, getting black specks into the product, leading to the reprocessing.	29
Figure S12. Univariate Trends between MSMPR1 PSD and Process Parameters: 24h PSD vs process parameters on the left. 30h PSD vs process parameters on the right.....	32
Figure S13. Univariate Trends between MSMPR2 PSD and Process Parameters.	33
Figure S14. Impact of τ , temperature, volume % ACN antisolvent, wt% API in the feed, API feed rate, and experiment duration on supersaturation in MSMPR1	34
Figure S15. Correlation of MSMPR 2 supersaturation with process variables.	35
Figure S16. API solubility in 90/10 THF/water as a function of temperature and volumes ACN antisolvent added. (a) 50-60 °C (b) 40 °C (c) 18-27 °C (d) 10 °C	61
Figure S17. Parity plots of experimental and model predicted values of X10, X50, and X90 in MSMPR1, MSMR2 and MSMPR3 using research scale experimental data. Filled symbols indicate entries used for estimation of parameter and open symbols indicate experiments used for validation of the model.	64
Figure S18. Parity plot of experimental and model predicted values of X10, X50, and X90 using pilot scale run data. Filled symbols indicate entries used for estimation of parameter and open symbols indicate experiments used for validation.....	65

List of Tables.

Table S1. Particle size distribution data for Experiment P3.....	29
Table S2. Particle size distribution data for experiment P4.....	29
Table S3. Particle size distribution data for Experiment P7.....	29
Table S4. Particle size distribution data for the 18 manufacturing batches. The repeat data points are repeat analyses of the same sample, not a separate sample.....	30
Table S5. Operating parameters used as independent variables in the modeling of particle size distribution data.	31
Table S6. Particle size distribution measurement for the research scale MSMPR experiments.	31
Table S7. Supersaturation for research scale MSMPR experiments.....	33
Table S8. RTD model elements and equations	51
Table S9: Population balance parameter value and variable descriptions for crystallization model 1.	62
Table S10. Model predictions of particle size after 30 h for base case conditions at manufacturing scale	66

1. Original batch process.

Prior to the development of the continuous crystallization process, the preceding cGMP campaign used a tech to final batch crystallization process. First, a rapid tech grade crystallization and filtration removed the dimeric impurity. Then, a final crystallization was done with slurry milling of the resulting purified solid. The batch approach was not viewed as a robust long-term option for kinetic impurity rejection because it is difficult to maintain the same timing of the tech grade crystallization and washing when scaling up.

The tech grade batch crystallization procedure was as follows:

1. begin with the crude API solution from aqueous workups
2. distill to <0.23 volumes water and <2.07 volumes of THF at atmospheric pressure
3. add THF and water to adjust to 0.23 volumes water and 2.07 volumes THF
4. polish filter at 60 C
5. THF/water rinse the polish filter with 0.09 volumes THF and 0.01 volumes water
6. cool to 50 C
7. add 2 volumes ACN
8. seed and then stir 1-3 h
9. add 7.2 volumes ACN over 6 h
10. cool to 10 C, then stir 6-8 h
11. filter, wash with 3 volume ACN, then wash with 3 volumes toluene twice
12. dry at 50-60 C

Final batch crystallization procedure was as follows:

1. begin with the tech grade API
2. add 0.23 volumes water and 2.07 volumes THF
3. heat to 60 C to for dissolution
4. cool to 48 C
5. add seed and then stir 1-3 h
6. add 9.2 volumes ACN over 6 h
7. cool to 10 C at 8 C/h, then stir 6-8h
8. slurry mill
9. monitor particle size, continuing milling until the d50 is 45-60 um
10. heat to 60 C then stir 6-7 h
11. cool to 10 C then stir 6-8 h
12. filter
13. wash with 3 volumes ACN, then wash with 3 volumes toluene twice
14. dry at 50-60 C
15. co-mill

2. Equipment and automation descriptions

2.a. Research scale systems

2 MSMPRs in series

A process flow diagram for the 2 MSMPRs in series system is shown in Figure S1. The crude API feed solution tank, process transfer tubing, and the transfer pump were all kept hot in the research scale experimental setup. This was accomplished by putting the feed vessel, the pump, the pump pressure relief valve, and all the connecting fittings inside the heated transparent polycarbonate enclosure maintained at about 55 °C, i.e. “hot box”. The tubing between the hot box and the crystallizer was jacketed and held at constant temperature of 50 °C.

The deltaV laboratory automation system ran the following sequence to transfer slurry from MSMR1 to 2, and from MSMR2 to the filter. Refer to Figure S1.

MSMR1 to MSMR 2

1. Close valve K (vent on MSMR2)
2. Open valve L (vacuum on MSMR 2) and Open valve M (Extra nitrogen supply to vent header to prevent air suck back from vent bubbler while vacuum is pulling on system). The first phase of the vacuum pull has enough magnitude to get the slurry up and over the hump in the arching tubing between vessels, overcoming gravity, and it is almost instantaneous. The second phase is a slower gradual vacuum pull that completes the transfer with minimal splashing or stripping.
3. Wait slurry transfer time (user input, example 2 seconds)
4. Close valve L
5. Open valve K
6. Close valve M
7. Wait remaining cycle time (example, the rest of the 12-minute cycle time)

Automated sequence to transfer slurry from MSMR2 to filter

1. Open valve D (nitrogen to pressure up transfer zone)
2. Wait for target pressure on transfer zone (user input, for example 900 torr)
3. Close valve D
4. Open valve A (valve between MSMR2 and transfer zone)
5. Wait time (user input, for example 2 seconds. This blows nitrogen back from transfer zone to MSMR2 to clear the line so that the subsequent slurry slug transferred will be representative of slurry in MSMR2)
6. Close valve A
7. Open valve C (pull vacuum on transfer zone)
8. Wait for target pressure on transfer zone (user input, for example 300 torr)
9. Close valve C
10. Open valve A (pulls slurry slug from MSMR2 into transfer zone by trapped vacuum)
11. Wait for target pressure on transfer zone (user input, for example 700 torr)
12. Close valve A
13. Open valve D (apply nitrogen pressure to the headspace of the transfer zone)
14. Wait for target pressure on transfer zone (user input, for example 1200 torr)
15. Open valve B (valve between transfer zone and filters)
16. Wait time (user input, for example 2 seconds. This pushes the slurry to the filters)
17. Close valve D
18. Close valve B
19. Open valve D (nitrogen to pressure up transfer zone)
20. Wait for target pressure on transfer zone (user input, for example 900 torr)
21. Close valve D
22. Open valve A
23. Wait time (user input, for example 2 seconds. This blows nitrogen back from transfer zone to MSMR2 to clear the line)
24. Close valve A

The transfer zone, used for transfers to the filter, is an intermediate pressure swing vessel with 4 automated block valves for slurry in (valve A), slurry out (valve B), vacuum (valve C), and nitrogen pressure (valve D). Vacuum is trapped in the zone, then it sucks slurry from the previous MSMR, and finally it pressurizes and pushes the slurry forward to the next vessel. Typically, an extra nitrogen push in the forward and reverse direction is done at the end to clear the tubing more thoroughly.

The vacuum transfer, on the other hand, pulls vacuum on the headspace of the process vessel that is receiving the slurry transfer. Therefore, achieving adequate seals on the agitator and all connections is essential for the pulling vessel (MSMR2) so that the system stays inert.

A potential negative consequence of using the vacuum transfer to move hot slurry from MSMR1 to 2 is that solvent can be stripped away, especially from the hot MSMR. Solvent stripping is minimized in three ways. First, the nitrogen supply to the vent system is pre-saturated with solvents. Second, the excess pull time from MSMR1 to 2 is minimized. Third, the vacuum pull is done in two phases, accomplished by vacuum pots, metering valves, and automated block valves. Excess gas blowing was minimized by the manually adjustable metering valve immediately upstream from the “Vacuum Knockout” vessel in Figure S1. The magnitude of the initial vacuum pull from MSMR1 to MSMR2 was set by the size of the vessels called “vacuum pots” in Figure S1. The vacuum pots were connected between the automated block valve L and the vacuum metering valve. With this arrangement, the slurry transfer experienced an immediate pull with just enough magnitude to transport the slurry slug up and over the hump in the arching tubing between MSMRs, followed by a slow metered pull to complete the slurry transfer from MSMR1 to 2 with minimum splashing or gas stripping. Average overall mass balance for research scale experiments was 98.1%, verifying that solvent stripping was minimized during the slurry transfers. This same method (vacuum pots and metering valve downstream from the vacuum block valve) was used at pilot and manufacturing scales as well.

Level control was achieved by the vertical position of the dip tubes used for slurry transfer. Each time slurry transferred out of an MSMR, the slurry operating volume returned to dip tube level. Complete solids suspension mixing was important because the slurry was pulled from the top portion of the operating volume. Therefore, baffling was extremely important to achieve flow in the axial direction which circulated the solids to the top. Each crystallizer used 4 flat baffles, with each baffle width about 1/10 of vessel diameter, extending down into the vessel as far as possible. Baffles were either glass or Teflon®. The Teflon® was “polished” as smooth as possible to, minimize the tendency of solids to stick. It is known that surface roughness can increase fouling.^{1,2} Tendency for solids to encrust on “polished” Teflon® surfaces and glass surfaces was similar; therefore, hydrophilic versus hydrophobic surface properties were not a dominating factor. Glass might have been slightly better for preventing encrustation, but it was easier to make custom baffle inserts out of polished Teflon® and seal and secure them in the MSMRs.

An alternative to controlling slurry level in the vessel at the dip tube would have been to push the dip tube down lower into the vessel, and use some other type of level control. A benefit of positioning the dip tube closer to the middle of the vessel is that non-uniform solids suspension becomes less of a problem. One of the fundamental assumptions of MSMRs is that slurry density and PSD in the outlet transfer tubes is representative of the bulk in the stirred vessel, and this is not achievable if the outlet tube is near the top and solids suspension is not 100% uniform from top to bottom. Nevertheless, the dip tubes were near the top of the MSMR for the level control benefits, and also because the MSMRs

were eventually operated with the transfer tube entering the next vessel sub-surface. Had the tube been sub-surface in both vessels, then a Tee and a valve would have been needed in the transfer tubing between vessels to clear the slurry line between transfers, which would have added complexity and propensity for solids clogging.

All feed tubes for the homogeneous solutions were 1.59 mm i.d. PFA tubing, and all transfer tubing for slurries was 3.96 mm i.d. PFA tubing. The slurry transfer tube from MSMPR1 to 2 was not heat traced or insulated, because it was not necessary given the high velocity slurry transfers. The key design feature for hot slurry transfer was that it was almost instantaneous. It only took about 2 s to transfer the entire slurry slug from MSMPR1 to MSMPR2; therefore, it did not have time to cool. The single piece of 3.96 mm i.d. PFA tubing forming a smooth arch from vessel to vessel with no fittings or flow restrictions was used to minimize the likelihood of solids clogging.

The MSMPR heating jackets were only filled with heat transfer oil on the lower part of the vessels, below target operating height. When the heat transfer fluid is above the liquid level, local evaporation of solvent occurs, establishing a gradient in the surface tension, that subsequently imparts interfacially driven flow. This is referred to as the Marangoni effect.^{3,4} During a crystallization, the Marangoni effect is undesirable as solute and crystals are transported with the flow of the anti-solvent rich liquid, causing API solids to gradually climb up the walls of the heated MSMPRs. The 250 mL glass vessels used for the MSMPRs had full height jackets, but a unique technique was used to make them operate like half-jackets. Heat transfer oil flowed in the bottom of the jacket and out the top, exiting the top of the jacket through a PFA dip tube that extended down into the jacket at the desired height. A small, metered flow of nitrogen was added to the vessel jacket as well, to maintain the nitrogen headspace above dip tube level in the jacket. The laboratory circulators were not sealed gas-tight, therefore the small amount of nitrogen flow could exit the circulator bath and not build up pressure in the hot oil loop.

3 MSMPRs in series

A process flow diagram for the 3 MSMPRs in series system is shown in Figure S2, and a picture of the 3 MSMPRs in series operating at research scale is shown in Figure S3.

Adding the third MSMPR required additional automation for intermittent slurry transfers between vessels. An automated block valve was added in the transfer tubing between MSMPR2 and MSMPR3 (valve J in Figure S2) to allow MSMPR2 head space to be isolated for vacuum and prevent slurry from going all the way to MSMPR3 during the transfer from MSMPR1 to MSMPR2. The new automated sequences for transferring slurry from MSMPR3 to the filters, MSMPR2 to MSMPR3, and MSMPR 1 to MSMPR2 once every 10 min are written in detail below.

Automated sequence to transfer slurry from MSMPR3 to the filters once every 10 minutes

1. Open valve D (nitrogen to pressure up transfer zone)
2. Wait for target pressure on transfer zone (user input, for example 900 torr)
3. Close valve D
4. Open valve A (valve between MSMPR3 and transfer zone)
5. Wait time (user input, for example 2 seconds. This blows nitrogen back from transfer zone to MSMPR3 to clear the line so that the subsequent slurry slug transferred will be representative of slurry in MSMPR3)

6. Close valve A
7. Open valve C (pull vacuum on transfer zone)
8. Wait for target pressure on transfer zone (user input, for example 300 torr)
9. Close valve C
10. Open valve A (pulls slurry slug from MSMR3 into transfer zone)
11. Wait for target pressure on transfer zone (user input, for example 700 torr)
12. Close valve A
13. Open valve D (apply nitrogen pressure to the headspace of the transfer zone)
14. Wait for target pressure on transfer zone (user input, for example 1200 torr)
15. Open valve B (valve Between transfer zone and filters)
16. Wait time (user input, for example 20 seconds. This pushes the slurry to the filters)
17. Close valve D
18. Close valve B
19. Open valve D (nitrogen to pressure up transfer zone)
20. Wait for target pressure on transfer zone (user input, for example 900 torr)
21. Close valve D
22. Open valve A
23. Wait time (user input, for example 2 seconds. This blows nitrogen back from transfer zone to MSMR3 to clear the line)
24. Close valve A

Automated sequence to transfer slurry from MSMR2 to MSMR3 once every 10 minutes

1. Close valve G (vent on MSMR3)
2. Open valve F (Vacuum on MSMR3) and Open A (Extra nitrogen supply to vent header to prevent air suck back from vent bubbler while vacuum is pulling on system). Valve J is already open.
3. Wait slurry transfer time (user input, example 10 seconds)
4. Close valve F
5. Open valve G
6. Close valve M
7. Wait remaining cycle time (example, the rest of the 10 minute cycle time)

Automated sequence to transfer slurry from MSMR 1 to MSMR2 once every 10 minutes

1. Close valve H (vent on MSMR2)
2. Close valve J (valve between MSMR 2 and MSMR 3)
3. Open valve E (vacuum on MSMR 2) and Open valve M (Extra nitrogen supply to vent header to prevent air suck back from vent bubbler while vacuum is pulling on system)
4. Wait slurry transfer time (user input, example 10 seconds)
5. Close valve E
6. Open valve H
7. Open valve J
8. Close valve M
9. Wait remaining cycle time (example, the rest of the 10 minute cycle time)

2.b. Pilot scale. 250 mL evaporator, three 2 L MSMPRs in series, and dual 250 mL agitated filters

A schematic diagram for the pilot scale evaporator, 3 MSMPR cascade, and automated dual filter are shown in Figure S4. This was the final equipment configuration for the pilot scale system, at the end of the development work which led to several design improvements. Pictures of the 250 mL continuous evaporator, 2 L MSMPRs, and 80 mm filters while running at steady state are shown in Figure S5.

Once every 10 min, a small portion of slurry was intermittently transferred from MSMPR3 to the filter, then from MSMPR2 to MSMPR3, then from MSMPR1 to MSMPR2, then from evaporator to MSMPR1. Automated sequence for slurry transfers out of each MSMPR was the same as described above for the research scale 3 MSMPRs system. Level control was achieved by the vertical position of the dip tubes used for slurry transfer. The slurry transfer tubes entering MSMPR 2 and 3 were subsurface. This minimized solid fouling and clogging at the end of the transfer tube. All slurry transfer tubes were 6.4 mm i.d. PFA tubing. The slurry transfers out of MSMPR1 and MSMPR2 were accomplished by vacuum. The automation system operated valves on a timed sequence. The automated valve sequence created pressure differences which intermittently pulled slurry from one vessel to another. Slurry transfer out of MSMPR 3 was done using a four-valve transfer zone. The slurry transfer systems and the tubing were selected and constructed in a way that minimized solid clogging. There were no local minimum heights in tubing flow paths between vessels so that the lines cleared after each transfer as completely as possible. Slurry transfer tubing between vessels was smooth and arching, up out of one vessel and down into the next to minimize clogging spots and so that slurry would gravity drain back into MSMPRs in both directions at the end of a transfer.

Evaporator.

The evaporator boiling pot was heated with a steam coil made from 1.59 mm o.d. tubing. The reason for selecting a heating coil was because a high surface area heating insert would be required when scaling up to manufacturing in order to have high enough boiling surface area per unit volume. Thus, a coiled tube was used to determine the heat transfer coefficient and to test for solids fouling on the stainless steel boiling coil. Steam heating provided an efficient way to deliver sufficient energy into the small diameter tubing. Figure S4 shows the location of the thermocouples (TT) on the steam inlet to the boiling coil and the condensed water out of the coil.

A stainless-steel shell and tube heat exchanger, 0.13 m² area, with a bundle of 55 tubes was used as a total condenser on the side of the evaporator. Distillate flow was into the top and out the bottom of the condenser. It is important to note the heat input to the evaporator must equal the heat taken out by the condenser for the system to work properly. The condensed distillate gravity flowed down into a vapor-liquid separator, with the bottom outlet connected to a distillate pump to continuously pump out distillate to a collection vessel (Figure S4). The upper part of the vapor-liquid separator was connected to the process vent. A second outlet at an intermediate elevation in the vapor-liquid separator was connected to a reflux pump. This pump was run at a higher-than-necessary flow rate and pumped a biphasic mixture of liquid and gas, so that distillate level did not accumulate and exit through the vent, even when distillation rates oscillated. As designed, boil-up was in excess, the rate of distillate removal was controlled by the distillate pump, and all excess boil-up was returned to the evaporator via the reflux pump.

The automation sequence for the evaporator was as follows (refer to Figure S4 for valve positions):

- Evaporator Valve A is N2
 - Evaporator Valve B is concentrated API solution to MSMPR1
 - Evaporator Valve C is Vent
1. Open Valve B
 2. Wait time #7, example 3 seconds (allows B-valve solvent flush to drain to evaporator by gravity)
 3. Close Valve C
 4. Open Valve A
 5. Wait time #1, example 4 seconds (hot, concentrated crude API feed solution transfers from evaporator to MSMPR1)
 6. Close Valve A
 7. Wait time #2 (pressure is vented)
 8. Enable Pressure HiHi alarm (pressure decrease in evaporator confirms that the transfer happened, because the only way for pressure to decrease is to push out the transfer tube to MSMPR1)
 9. Open Valve C
 10. Close Valve B
 11. Wait time #3, example 5 seconds
 12. Open Valve B (to allow any residual concentrate in the line above B-valve to drain back to the evaporator by gravity)
 13. Wait time #4, example 3 seconds
 14. Close Valve B
 15. Wait time #5, example 3 minutes
 16. Open Valve B (allow the B-valve flush to drain to the evaporator)
 17. Wait time #6, example 3 seconds
 18. Close Valve B
 19. Wait the rest of the total sequence time (for example the rest of the 10 min).

Pilot scale startup procedures.

The purpose for the experiment P11 was to test the startup procedures for the evaporator, with emphasis on controlling the amount of foaming. Foaming had been observed during the initial concentration step in previous experiments. A start up process was needed that minimized the chance of the contents foaming out of the evaporator into the overhead condenser and distillate receiver. Three procedures evaluated were: (1) start boiling with the evaporator filled with THF, then start feeding crude API solution while boiling at total reflux and gradually concentrate contents in evaporator (2) start boiling with the evaporator filled with 5% water in THF, then start feeding crude API solution while boiling at total reflux and gradually concentrate contents in evaporator, and (3), start boiling with the evaporator filled with normal crude API feed solution, then start feeding crude API solution while boiling at total reflux and gradually concentrate contents in evaporator. The least amount of foaming was observed using the startup with the evaporator filled with normal crude API feed solution. Comparison photos of the three startup procedures are given in Figure S6.

With the least amount of foaming observed when starting from crude API feed solution, the startup procedure was designed as follows. The evaporator was filled to $\frac{1}{2}$ the operating volume with crude API feed solution, then heated to reflux. Then, THF and crude API feed solution started flowing at the target steady state feed rates. At the same time, the distillate pump was started at a rate equal to the combined total of the THF and crude API feed solution flowrates. These conditions maintained the volume in the evaporator at $\frac{1}{2}$ normal operating volume while the contents were gradually concentrated to ~25 wt% API. The chance of any foaming reaching the overheads of the evaporator were reduced because of the reduced operating volume in the evaporator. Once the evaporator bottoms reached ~25 wt% API, the distillate flow was reduced to the target steady state flow rate and the evaporator was allowed to gradually fill to the target operating volume. Once at the target operating volume, transfers to MSMR1 started. Foaming also occurred as the evaporator contents transitioned from concentrated API to solvent only during cleanouts. To minimize the chance of bumping to distillate during cleanout, the heat was reduced to provide only minimal reflux during shutdown transition.

2.c. Manufacturing scale continuous distillation in the development lab

A schematic diagram for the manufacturing scale evaporator tested in development labs is shown in Figure S7. The boiling pot had a 5 L operating volume. It was jacketed and it also had internal heating coils to maximize the heat transfer surface area per unit volume. The internal double heating coil was fabricated from 12.7 mm o.d. X 10.9 mm i.d. stainless steel tubing. The outer coil was 114 mm i.d. and the inner coil was 64 mm i.d. The height of each coil was 510 mm with 6 mm spacing. A 6 kW circulator was used for heating. Heat transfer fluid from the circulator flowed through the internal heating coils to the evaporator jacket which were connected in series.

At the start of each experiment, the evaporator was filled to the desired operating volume with THF (~3 L). The evaporator was heated to reflux with the vent pressure set at -0.7 psig. The flow process was started by continuously pumping crude API feed solution and THF into the evaporator and continuously pumping distillate to waste, until the evaporator contents were concentrated to above 20 wt% API, which took about 75 min. After the concentration was reached, the system was switched over to total recycle mode. In this mode, the distillate was pumped into the same stirred receiving vessel as the concentrated API. Material was continuously pumped from this stirred receiving vessel back into the evaporator as dilute API feed. The THF feed was not used when the process was run in total recycle mode. The baseline feed rate during the testing was 220 g/min crude API feed solution, but feed rates were investigated over the range 150 to 290 g/min.

Two Tees were installed just to the right of Valve A, one on each side of the top of the arch, shown in Figure S7. THF/water slowly dripped into each Tee to prevent solids fouling. On the evaporator side of the arch, the THF/water pumped at a rate of about 1 mL/min, pooled on the top of Valve A, and periodically drained back down into the evaporator when Valve A briefly opened about once every 3 minutes. This served to prevent solids from building up in Valve A. On the MSMR side of the arch, the THF/water constantly dripped and drained by gravity down into the MSMR vessel. The THF/water flow to the MSMR side was only 0.2 mL/min, so that it would have a minimal dilution effect on the transferred API concentrated solution, which flowed at an average of about 30 mL/min from the evaporator into the MSMR. Note that there was no crystallization in the MSMR for these tests.

Three different total condensers were tested. Two of the condensers were shell and tube heat exchangers, one with the internal tube bundle about 0.3 m long and a total heat transfer surface area of 0.8 m², and the other with internal tube bundle about 1 m long and a total heat transfer surface area of about 1 m². The third condenser was custom made from 19 mm o.d. 15.7 mm i.d. tube inside 25.4 mm o.d. 22.1 mm i.d. tubing, 5 m long, and 0.08 m² surface area.

The manufacturing scale experiments confirmed that the overall heat transfer coefficient for the boiling coils was ~300 W/m²K. For example, one set of the steady state operating parameters was:

- Temperature of heat transfer oil into the boiling coil (called “hot oil supply” in the figures) = 88 °C
- Temperature of heat transfer oil out of boiling coil (called “hot oil intermediate” in the figures) = 70 °C
- process temperature in the evaporator = 64 °C
- surface area of submerged coils when operating with 3 L fill level = 0.69 m²
- heat transfer oil mass flow rate = 8.3 kg/min

From this condition, the overall heat transfer coefficient for the boiling coils was about 280 W/m²K.

2.d. cGMP manufacturing

Evaporator

Intermittent flow of solution from the evaporator to the crystallizer was accomplished by the following automated valve sequence. Refer to Figure S8 for the valve locations.

1. Open A, Wait Time (USER INPUT TIME, example 3 seconds)
2. Close C, Open B, Wait time (USER INPUT TIME, example 3 seconds) for push from evaporator to crystallizer
3. Close B, Wait time (USER INPUT TIME) for evaporator to depressurize
4. Check pressure interlock to make sure not clogged between evaporator and crystallizer
5. Open C, Close A, Wait time (USER INPUT TIME, example 5 seconds)
6. Open A, Wait time (USER INPUT TIME, example 2 seconds) to drain back liquid to evaporator from outlet piping
7. Close A, Wait time (USER INPUT TIME, example 5 seconds)
8. Open A, Wait time (USER INPUT TIME, example 2 seconds) second drain back to clean valve A
9. Close A, Wait time (USER INPUT TIME, example 300 seconds)
10. Open A, Wait time (USER INPUT TIME, example 2 seconds) third drain back to clean valve A
11. Close A, Wait the remainder of the total cycle time (for example the rest of the 10 min)

Automated Valve A in Figure S8, between the evaporator and the crystallizers, prevented distillate from boiling into the crystallizers and also prevented suck back of headspace gas from the crystallizers into the evaporator. Note that the entry tube into MSMPR1 was above surface, or it would have sucked back slurry to the evaporator when Valve A opened for the periodic automated drain-backs.

As described for the 5 L development mode evaporator, the manufacturing plant evaporator was heated via a jacket and stainless-steel heating coils inside the unit. Evaporator jacket heating oil supply

temperature was normally about 83°C, and jacket oil return temperature was about 77°C. A 6 kW circulator was used for the jacket and internal heating coils. The evaporator internal process boiling point temperature was about 66°C when the evaporator pressure was about -0.5 psig.

Initially there was a constant low flow of 95/5 v/v THF/water at 7 g/min that was applied to the top of valve A, on the evaporator side of the arch. The automated sequence cycled valve A periodically to allow for solvent flushing of valve A by gravity. This was abandoned about 1/3 of the way through the manufacturing campaign because the pump was needed elsewhere. This was fortuitous because it proved that the valve solvent flush was not needed. Valve A remained clean and did not clog with solids.

Boiling point temperature was a stable hold for the crude API solution in the evaporator. The pilot scale experiments had proven stable hold points for 6 days in the evaporator at 64 °C and 21 days in the MSMPRs at 25 °C, which were the limits of knowledge at the time.

Evaporator startup with no diverting to waste

The intention was to keep all startup transition material for cGMP use. The evaporator began empty and was started up semi-batch. The dip tube for flow out of the evaporator was set to 5.5 L. First, 3 L of crude API feed solution was added to the evaporator, and the heat was started until the solution was boiling. All distillate was pumped back as total reflux from the condenser to the boiling pot. Then the crude API feed solution and THF flows were started at the target steady state flow rates, and the distillate flow was set equal to the two feeds so that level would remain constant at about 3 L in the evaporator while it was concentrating, to allow room for potential foaming. After long enough flow time to concentrate contents in the evaporator pot to 25 wt% API, the distillate mass flow rate was adjusted to target steady state value. The liquid level in the evaporator gradually rose to 5.5 L because no flow was going to MSPR1 yet. After reaching 5.5 L with 25 wt% API in the evaporator, the intermittent transfers to MSMPR1 and the ACN flow to MSMPR1 commenced.

Solvent recovery considerations

If this process were to scale up further in manufacturing, implementing solvent recovery from the distillation tank may be considered. The business case and environmental considerations would determine if solvent recovery was necessary. Solvent recovery for small volume processes may not make sense. Solvent recovery for larger volume processes would likely be done in batch. Our solvent recovery subject matter experts tell us solvent recovery is only viable when the solvent to be recovered is very expensive and a third party will take the material and execute the recovery, or when the process exceeds 25,000 kg/y API production rate. The capital cost of the recovery equipment and associated holding tanks is hard to justify in manufacturing.

3 MSMPRs in series

The automated sequence to transfer slurry from MSMPR 1 to MSMPR2 once every 10 minutes was as follows (refer to Figure S9).

1. Close valve B (vent on MSMPR2)
2. Close valve F (valve between MSMPR 2 and MSMPR 3)
3. Open valve C (vacuum on MSMPR 2) and Open valve A (Extra nitrogen supply to vent header to prevent air suck back from vent bubbler while vacuum is pulling on system. Note that the

metering valve in series with valve A is adjusted so that the extra nitrogen bubbling during transfer is sufficient to prevent suck back from the bubbler but not excessive. If it is excessive, then it requires more frequent top up of the Galden in the bubbler)

4. Wait slurry transfer time (user input, example 10 seconds. This timing was an important manual adjustment. Time must be long enough so that slurry transfers are complete, i.e. slurry level in the leaving vessel gets down to dip tube level, and the transfer tube clears. However, time must not be too excessive because that would result in slurry splashing in the receiving vessel, and also extra stripping of process solvents. Splashing would cause solids fouling on the wall and up on the head. Additionally, splashing was controlled by manually adjusting the metering valve in series with valves E and C.)
5. Close valve C
6. Open valve B
7. Open valve F
8. Close valve A
9. Wait remaining cycle time (example, the rest of the 10 minute cycle time)

Automated sequence to transfer slurry from MSMR2 to MSMR3 once every 10 minutes. Valve F is already in the open position.

1. Close valve D (vent on MSMR3)
2. Open valve E (Vacuum on MSMR3) and Open A (Extra nitrogen supply to vent header to prevent air suck back from vent bubbler while vacuum is pulling on system)
3. Wait slurry transfer time (user input, example 10 seconds)
4. Close valve E
5. Open valve D
6. Close valve A
7. Wait remaining cycle time (example, the rest of the 10 minute cycle time)

Automated sequence to transfer slurry from MSMR3 to the filters once every 10 minutes was part of the dual filter sequence as described in the next section.

The transfer zone pulled slurry from MSMR3 by trapped vacuum and then pushed it to the filters by nitrogen pressure, and it completed an extra nitrogen push in the reverse direction at the end to clear the tubing more thoroughly. The vacuum transfer was used to move slurry from MSMR1 to MSMR 2, and from MSMR 2 to MSMR 3. The vacuum transfer method pulled vacuum on the headspace of the process vessel that was receiving the slurry transfer. Therefore, achieving adequate seals on the agitator and all connections was essential for the pulling vessels so that the system remained inert. A potential negative consequence of using the vacuum transfer to move hot slurry between MSMRs was that solvent could be stripped away. Solvent stripping was minimized in three ways. First, the nitrogen supply to the vent system was pre-saturated with solvents. Second, the excess pull time between MSMRs was minimized. Third, the vacuum pull was done in two phases, accomplished by vacuum pots, metering valves, and automated block valves. The magnitude of the instantaneous initial vacuum pull was set by the size of vacuum pots, and the rate of the of the secondary vacuum pull was limited by metering valves in the vacuum line. Once every 10 minutes, when slurry transferred out of each MSMR, the operating volume inside the MSMR returned to dip tube level. One of the potential consequences of this mode of operation, with the dip tubes positioned at the top of the slurry level was that PSD of the

crystals exiting the transfer tubes might not be the same as average PSD in the bulk of the stirred vessel. An alternative was to position the dip tube down lower into the vessel and use some other type of level control. The slurry transfer would not empty the vessel all the way to the dip tube, and the transfer frequency would be governed by a radar level indicator. A benefit of positioning the dip tube closer to the middle of the slurry level is that non-uniform solids suspension becomes less of a problem. Nevertheless, for the manufacturing campaign described herein, the dip tubes were near the top of the MSMPR for the level control benefits, and also because the MSMPRs operated with the transfer tube entering the next vessel sub-surface. Had the tube been sub-surface in both vessels, then something like a Tee and a valve would have been needed in the transfer tubing between vessels to clear the slurry line between transfers.

The transfer tubes were flexible, and they were allowed to bend in flow. Furthermore, a small amount of movement of the ½" outer diameter PFA dip tubes was visible at various agitation rates, but the movement was limited because the dip tubes were positioned on the outside of the supporting baffle rings and near the front side of the flat baffle, therefore there was not much room to move.

Dip tube levels were set manually using calibrated level markings. Level sensors were installed higher in each vessel, with automated interlocks.

Agitators were 3-flight pitched blade turbines with a 150 mm diameter typically operating at 200 rpm. The lower impeller was about 75 mm above the bottom of the reactor, and the upper impellers were about 150 mm above each other. The shafts and impellers were PFA coated stainless steel. Custom baffle cages had 4 flat baffles with a width about 1/10 of the tank diameter. The baffle cage structure was fabricated from stainless steel and electropolished, and the baffles themselves were flat, polished Teflon® strips, attached to the metal by electropolished nuts and bolts with as few rough edges as possible. Solids fouling was a little less on glass surfaces compared to metal, Teflon, and PFA. Comparing metal, Teflon, and PFA, the influence of these 3 materials of construction on fouling was minimal.

Dual slurry-off filtration

The system was designed to move slurry. Minimum inside diameter was 0.95 cm for all slurry transfer tubing and valves by the end of the campaign. It did not all start out that way, but it was all changed to 0.95 cm i.d. by the end of the campaign in response to clogging events.

Filtration Skid Automation (SK 27) (refer to Figure S10).

Transfer to filter- SK 27 Operation **UT (Define cycle time)**

- Open W **UT (1 second)**
- Close W (blowback)
- Open X **UT (1 second)**
- Close X
- Open 'Lead Filter' Filtrate (S or T)
- Open V (pull vac) **UP PT SK27A**
- Close V
- Open X (pull slug) **UP PT SK27A (>-X.X psig)**
- Close X

- Open W (pressure) **UP PT SK27A (>0 psig)**
- Open Y (out) **UT**
- Close W
- Close Y
- Open W (blowback) **UT (1 second)**
- Close W
- Open X **UT**
- Close X
- Open 'Lead Filter' Nitrogen (D or E)
- Close 'Lead Filter' Nitrogen (D or E) **UT**
- Close 'Lead Filter' Filtrate (S or T)
- Count Shot +1

Calculate wait time from difference between total sequence time (user input) and the time this just took. A is duty filter until filter shot # = setpoint.

A Duty, B Standby

- Open F to Filter A
- Close J to Filter A
- Open S to filtrate waste
- Open T to Filter B
- Open M to Filter B
- Open E to Filter B **UT**
- Close E to Filter B **UP PT SK27C (<2 psig)**
- Open K to Filter B
- Close T to Filter B
- Open B to Filter B (Charge Wash) **UV FT SK27B (XX Liters)**
- Close B to Filter B
- If stirring is selected, Open P Out
- Close P
- Close K to Filter B
- Open T to Filter B
- Open A to Filter B **UT**
- Close A to Filter B **UP PT SK27C (<2 psig)**
- Close M to Filter B
- Close T to Filter B
- Open K to Filter B
- Open H to Filter B (Charge slurry off) **UV on FT SK27A (XX Liters)**
- Close H to Filter B
- Open P to Filter B (Agitation) **UT**
- Close K to Filter B
- Open E to Filter B **UP PT SK27C (>2 psig)**
- Open Valve AC to Filter B (Slurry Receiver) **UT**

- Close P to Filter B
- Close E to Filter B
- Open K to Filter B
- Open H to Filter B (Charge rinse) **UV on FT SK27A (XX Liters)**
- Close H to Filter B
- Close K to Filter B
- Open E to Filter B **UT**
- Close E to Filter B
- Close Valve AC to filter B
- Open K to Filter B
- Open M to Filter B
- If Rinse Selected: Open C to Filter B (Charge Clean) **UV FT SK27B (XX Liters)**
 - Close C to Filter B
 - Close K to Filter B
 - Open P to Filter B UT
 - Close P to Filter B UT
 - Open T to Filter B
 - Open A to Filter B **UT**
 - Close A to Filter B **UP PT SK27C (<2 psig)**
 - Close M to Filter B
 - Close T to Filter B
- Purge: Close K to filter B
- Open T to Filter B
- Open E to Filter B UT
- Close E to Filter B
- Close T UP PT SK27C
- Cycle Wait

B Duty, A Standby

- Open F to Filter B
- Close K to Filter B
- Open T to filtrate waste Filter B
- Open S to Filtrate Waste Filter A
- Open L to Filter A
- Open D to Filter A **UT**
- Close D to Filter A **UP PT SK27B (<2 psig)**
- Open J to Filter A
- Close S to Filter A
- Open B to Filter A (Charge Wash) **UV FT SK27B (XX Liters)**
- Close B to Filter A
- If stirring selected, Open N **UT**

- Close N
- Close J to Filter A
- Open S to Filter A
- Open A to Filter A **UT**
- Close A to Filter A **UP PT SK27B (<2 psig)**
- Close L to Filter A
- Close S to Filter A
- Open J to Filter A
- Open G to Filter A (Charge Slurry off) **UV on FT SK27A (XX Liters)**
- Close G to Filter A
- Open N to Filter A (Agitation) **UT**
- Close J to Filter A
- Open D to Filter A **UP PT SK27B (>2 psig)**
- Open Valve AB to Slurry Receiver **UT**
- Close N to Filter A
- Close D to Filter A
- Open J to Filter A
- Open G to Filter A (Charge rinse) **UV on FT SK27A (XX Liters)**
- Close G to Filter A
- Close J to Filter A
- Open D to Filter A **UT**
- Close D to Filter A
- Close Valve AB to Filter A
- Open J to Filter A
- Open L to Filter A
- If Rinse selected: Open C to Filter A (Charge Clean) **UV FT SK27B (XX Liters)**
 - Close C to Filter A
 - Close J to Filter A
 - Open S to Filter A
 - Open A to Filter A **UT**
 - Close A to Filter A **UP PT SK27B (<2 psig)**
 - Close L to Filter A
 - Close S to Filter A
- Purge: Close J to Filter A
- Open S to Filter A
- Open D to Filter A **UT**
- Close D to Filter A
- Close S **UP PT SK27A**
- Cycle Wait

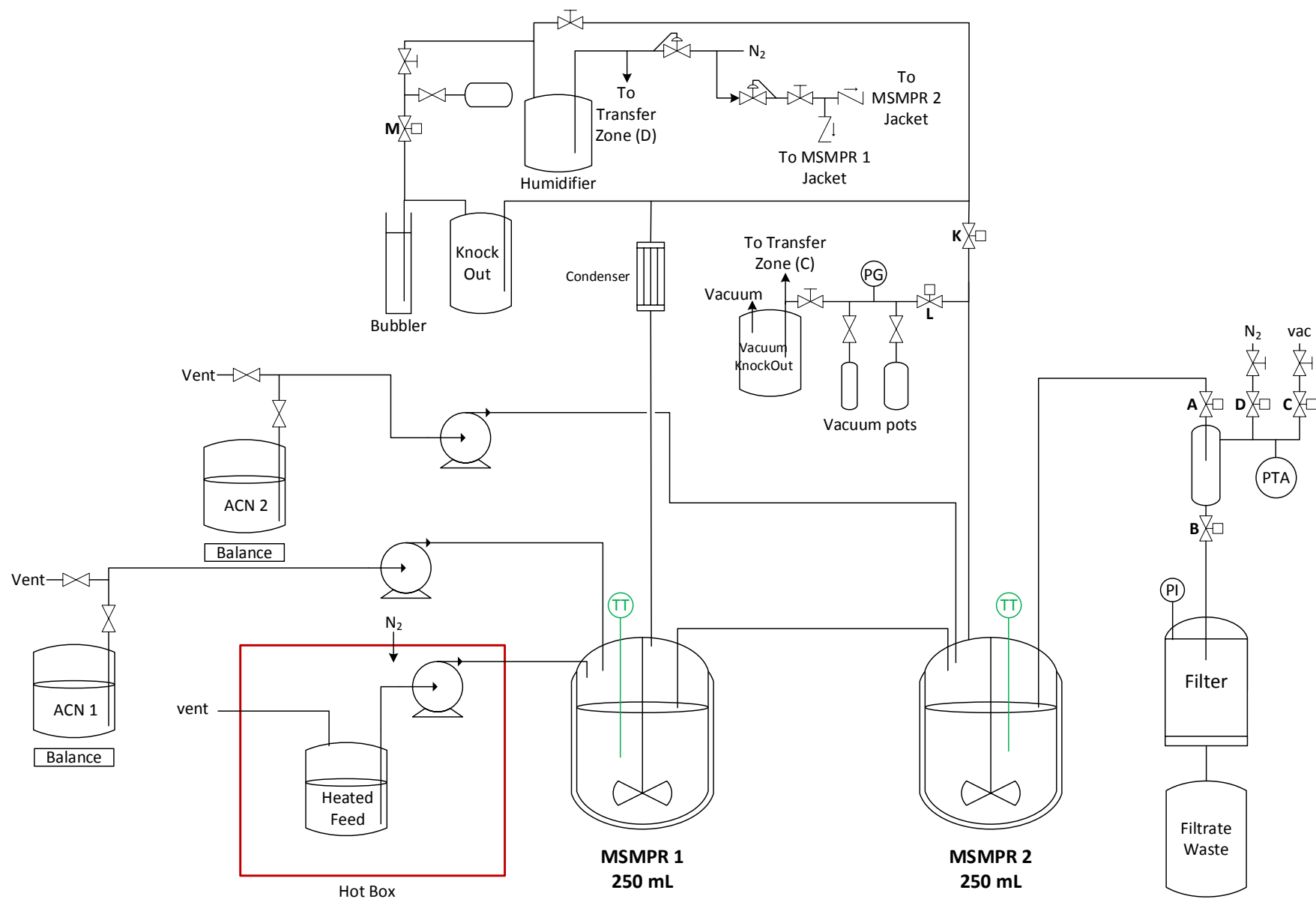


Figure S1. Schematic for 2 MSMPRs in series system.

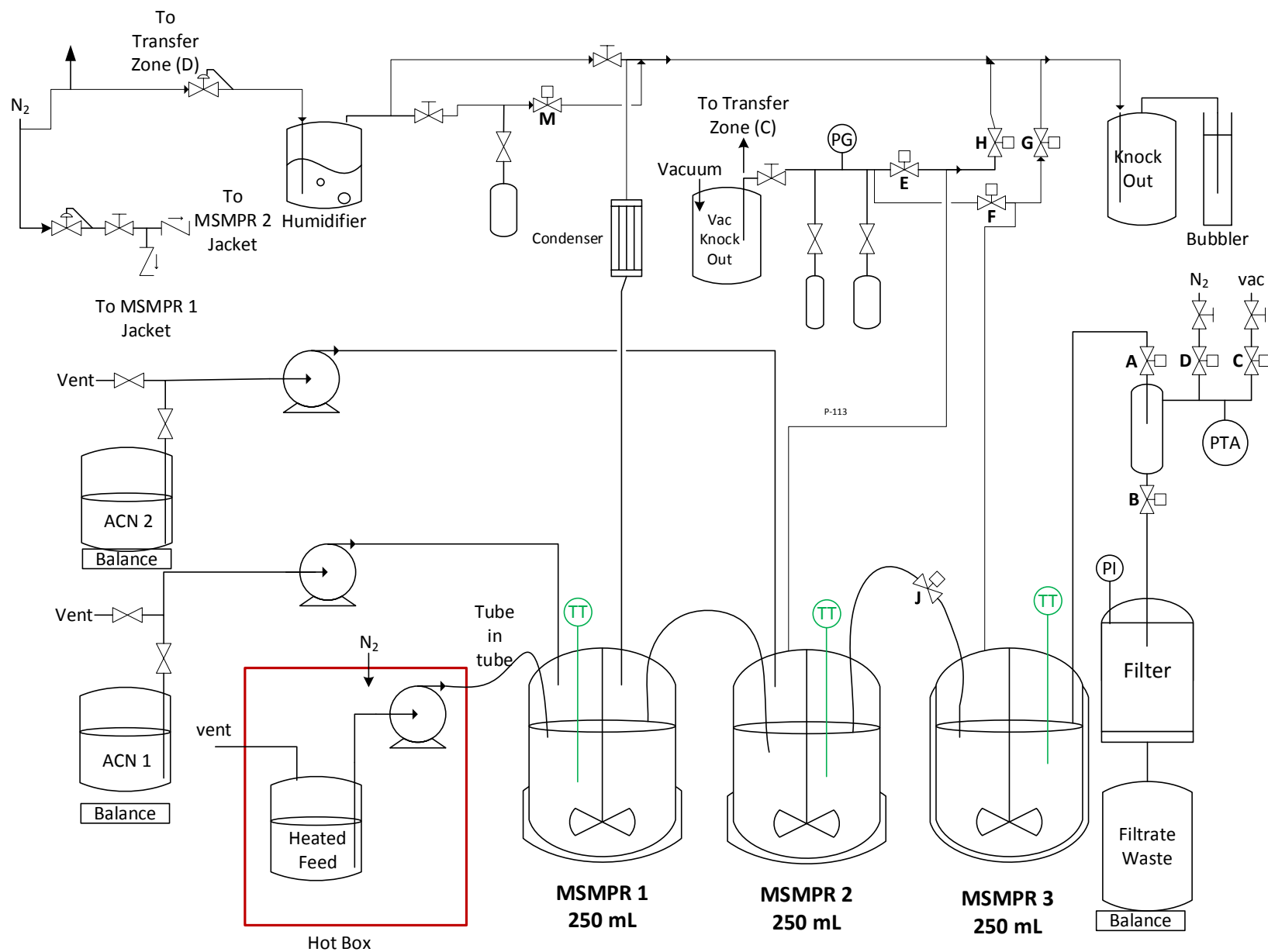


Figure S2. Schematic for 3 MSMPRs in series at research scale.



Figure S3. Picture of the 3 MSMPRs in series operating at research scale, MSMPR1, 2 and 3 from left to right.

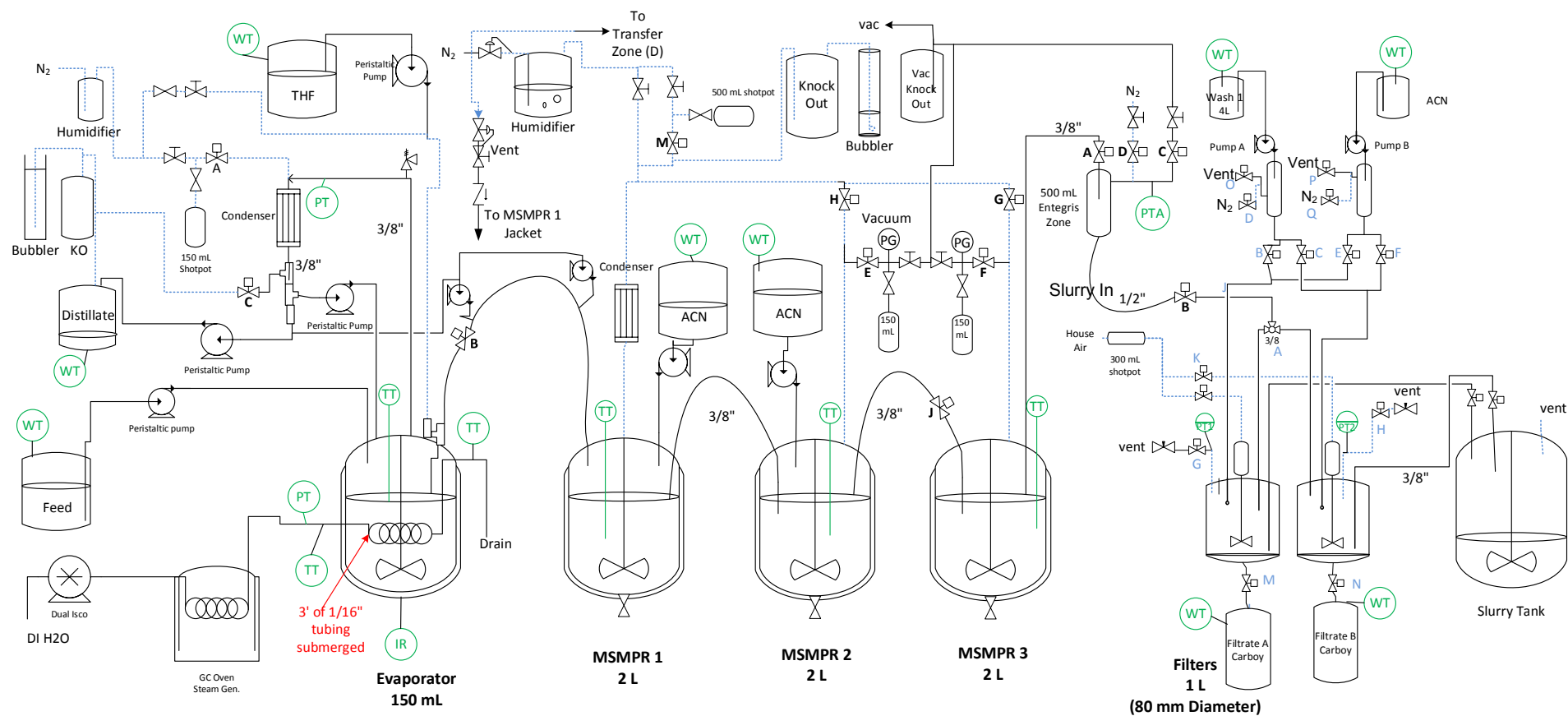
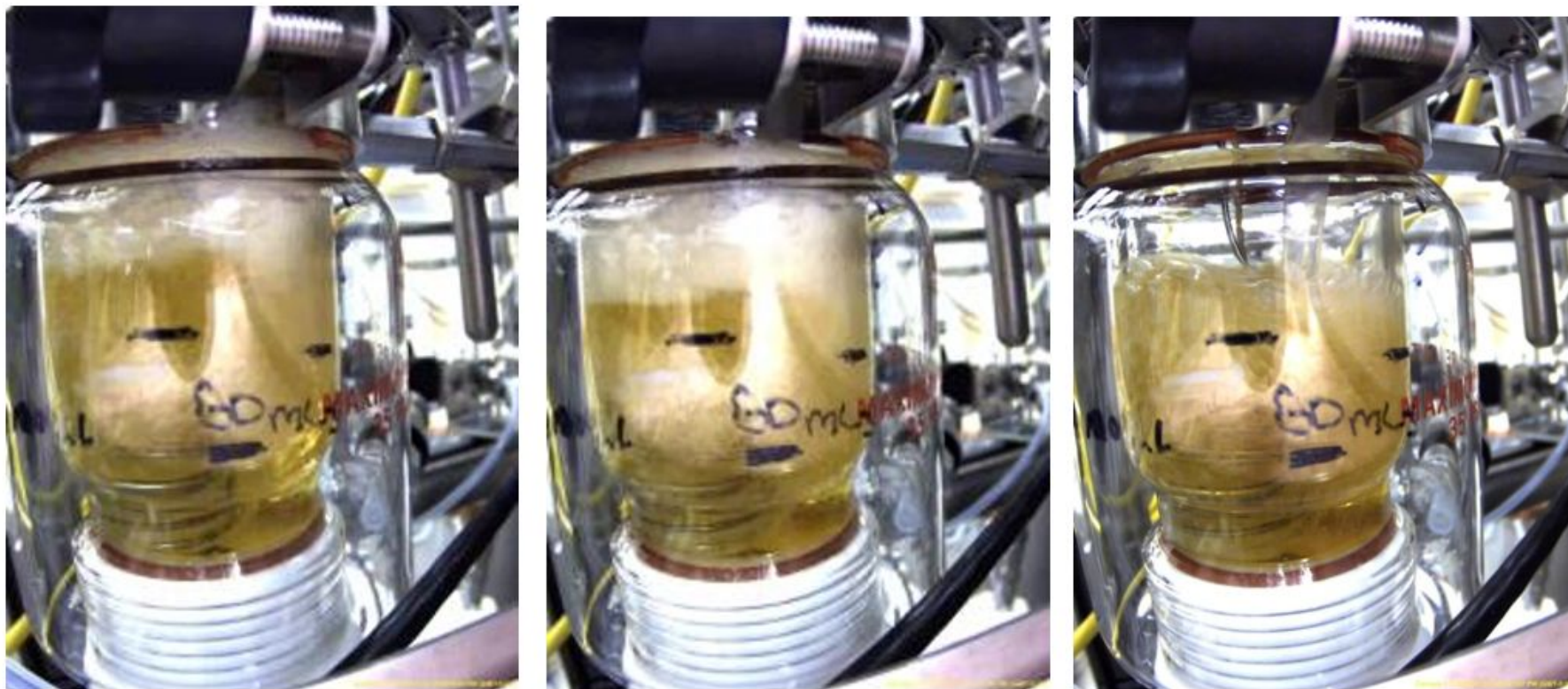


Figure S4. Schematic diagram for the 250 mL evaporator, three 2 L MSMPRs in series, and 80 mm diameter jacketed glass dual slurry-off filters.



Figure S5. Picture of the 250 mL continuous evaporator, three 2 L MSMPRs, and one of the dual slurry-off filters while running at steady state.



(a, b, and c, left to right)

Figure S6. Foaming after the first 15 min running the evaporator. (a), Evaporator started refluxing with only THF. (b), evaporator started with 95/5 THF/water v/v. (c) evaporator started with representative crude API feed solution.

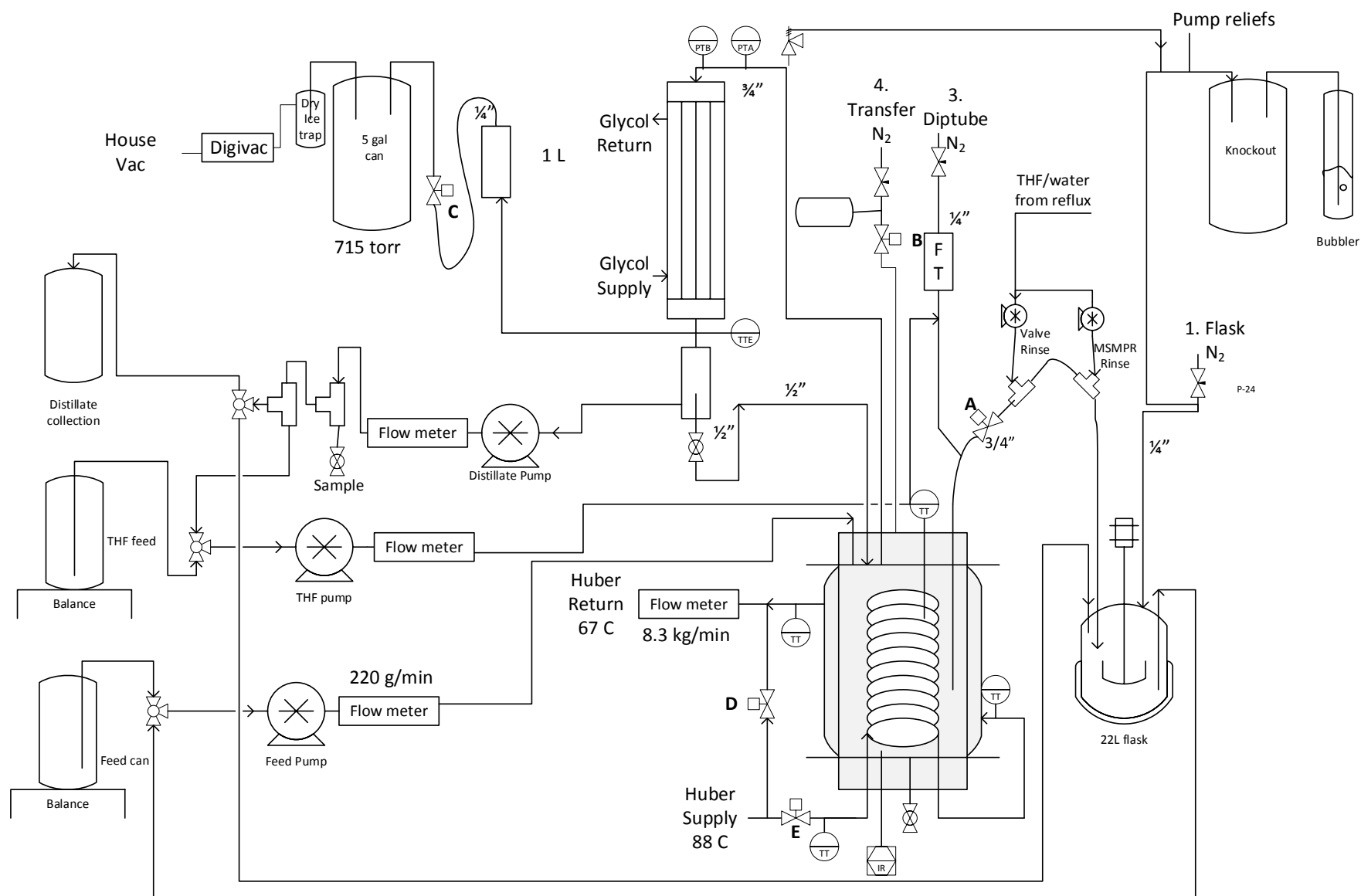


Figure S7. Process diagram for manufacturing scale evaporator tested in development labs.

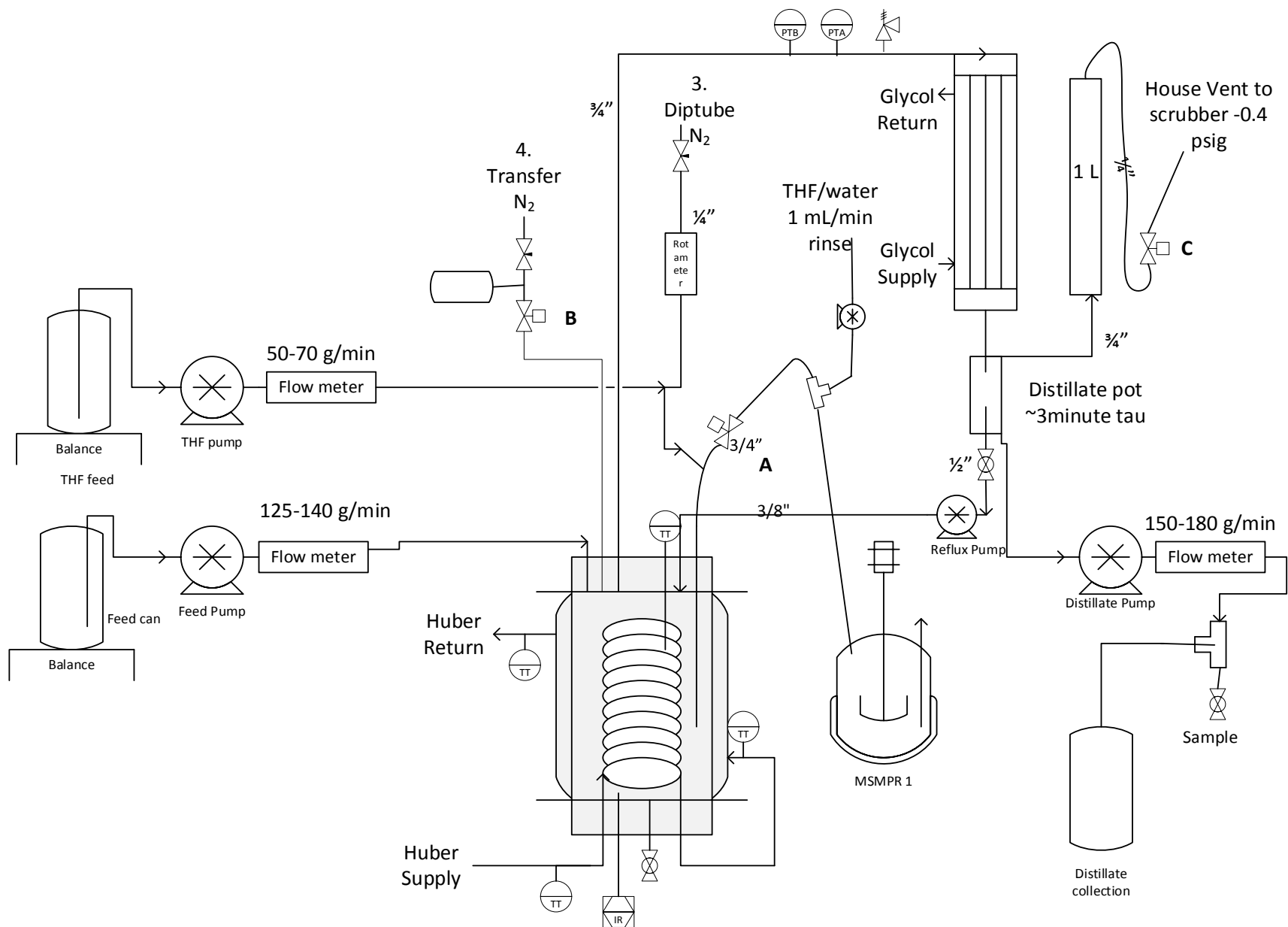


Figure S8. Schematic of the cGMP manufacturing plant evaporator.

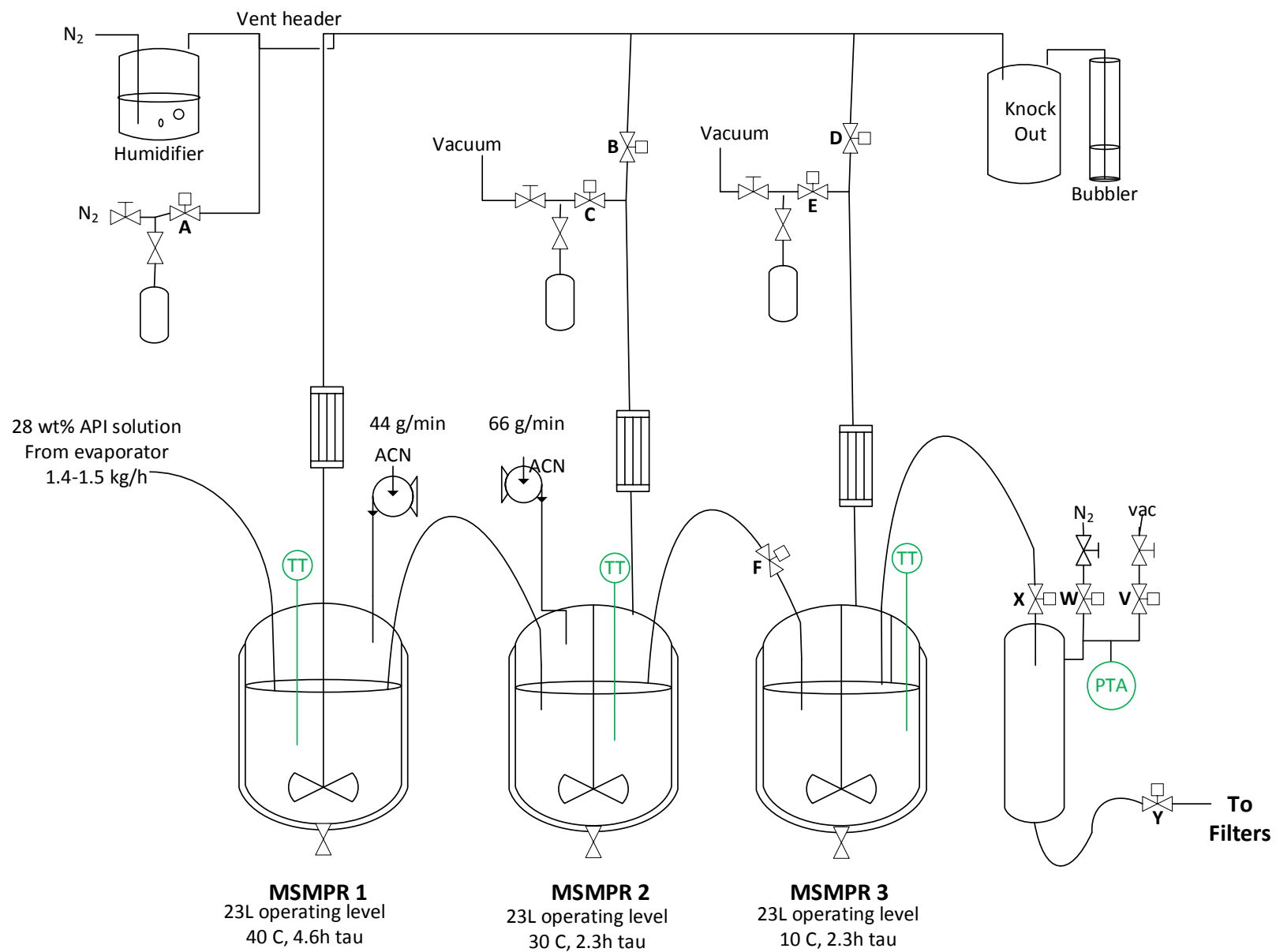


Figure S9. Schematic of the cGMP manufacturing plant MSMPRs in series.

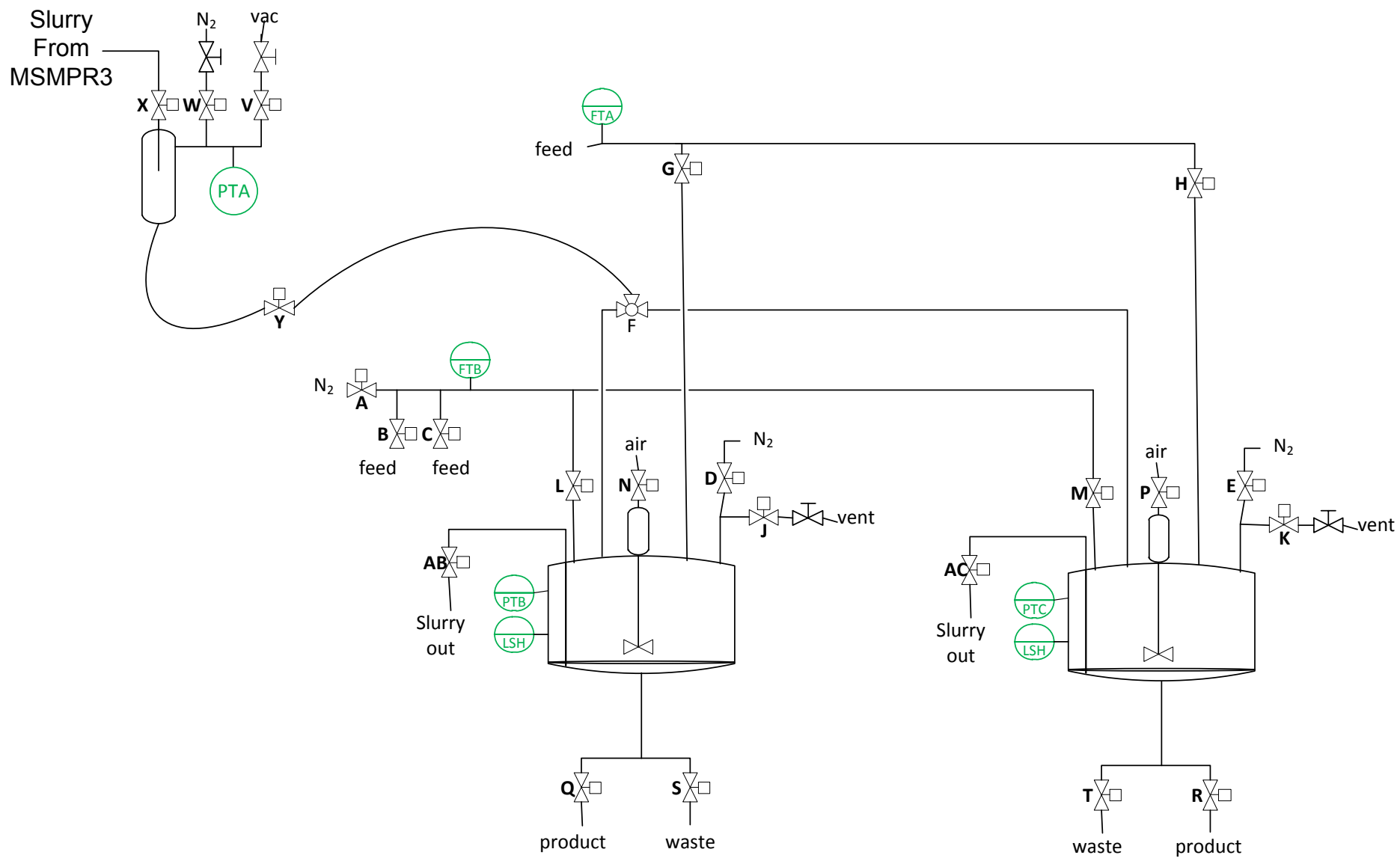


Figure S10. Schematic of dual filter skid in manufacturing.

Preventing particulates from the agitator seals was of utmost importance, and it was the reason that the first four batches needed to be re-processed. The black bits were from the O-rings shown in a picture in Figure S11.



Figure S11. Filter agitator seals used at the beginning of the campaign. These are the O-rings that shed, getting black specks into the product, leading to the reprocessing.

After the first four batches the seals were replaced with versions that were non-shedding.

3. Particle Size Distribution Data

Table S1. Particle size distribution data for Experiment P3

	MSMPR1			MSMPR2			MSMPR3		
sample description	x_{10} (μm)	X_{50} (μm)	X_{90} (μm)	x_{10} (μm)	X_{50} (μm)	X_{90} (μm)	x_{10} (μm)	X_{50} (μm)	X_{90} (μm)
after 24 h flow time	47	268	570	46	252	537	39	246	498
after 45 h flow time	50	164	454	53	163	440	47	149	394
after 48 h flow time	53	178	523	55	174	482	50	160	406

Table S2. Particle size distribution data for experiment P4.

	MSMPR1			MSMPR2			MSMPR3		
Sample time (h)	x_{10} (μm)	X_{50} (μm)	X_{90} (μm)	x_{10} (μm)	X_{50} (μm)	X_{90} (μm)	x_{10} (μm)	X_{50} (μm)	X_{90} (μm)
12	71	322	530	142	311	538	149	285	488
23	53	175	656	52	219	714	49	203	668
28	63	177	566	59	166	594	58	157	653

Table S3. Particle size distribution data for Experiment P7.

	MSMPR1			MSMPR2			MSMPR3		
--	--------	--	--	--------	--	--	--------	--	--

sample description	x10	x50	x90	x10	x50	x90	x10	x50	x90
end of filling	123	261	447	91	204	356	130	243	418
after hold still warm	111	281	470	107	209	360	104	195	340
after hold and cool	58	269	479	122	245	419	127	245	423
after 20 h flow time	74	190	387	81	204	435	67	169	390
end of run and overnight stir	32	105	362	39	169	428	37	156	410

Table S4. Particle size distribution data for the 18 manufacturing batches. The repeat data points are repeat analyses of the same sample, not a separate sample.

batch	x10 (um)	x50 (um)	x90 (um)	obscuration, %
1	169	337	572	20
1	169	337	573	19.7
2	49	281	645	16.8
2	47	278	656	19.3
3	94	356	729	15.7
3	93	353	738	15.9
4	24	142	597	17.3
4	24	143	556	17.9
5	64	316	589	17.6
5	61	311	595	15.7
6	46	194	484	17.2
6	70	276	565	17.6
7	61	290	539	16.3
7	81	299	545	17.1
8	40	185	490	18.7
8	41	181	507	17
9	64	293	619	19.6
9	61	277	576	20.2
10	43	255	596	16.7
10	40	247	607	21.4
11	85	309	608	16.8
11	91	315	612	16.1
12	45	242	562	16.9
12	40	228	538	21.2
13	80	222	418	15.7
13	83	229	425	18.8
14	89	329	632	16.9
14	93	336	643	17
15	61	256	557	18.3
15	87	319	622	16.4
16	72	307	605	25.4
16	73	304	605	25.4
17	61	265	575	17.8
17	57	260	587	21.2
18	50	233	566	21.7
18	49	237	553	19.7

4. Exploratory Data Analysis

4.a. Research scale PSD

The research scale experiments R3-R11 covered a range of conditions including MSMPR1 temperature 25-50 C, vol% ACN in MSMPR1 solvents 65-88%, vol% ACN in MSMPR2 solvents 79-90%, and API feed 24-27 wt% (Table S5).

Table S5. Operating parameters used as independent variables in the modeling of particle size distribution data.

Experiment	wt% API in the feed	target feed solvents THF/water v/v	vol% ACN in solvents in MSMPR1	vol% ACN in solvents in MSMPR2	MSMPR1 temp, °C	MSMPR1 τ , h	MSMPR2 τ , h
R3	27	90/10	80	80	25	4	4
R4	24	90/10	79	79	40	4	4
R5	24	90/10	88	88	25	2.6	2.6
R6	24	90/10	65	79	25	6.4	4
R7	24	90/10	67	87	40	6	2.4
R8	25.2	89/11	68	88	40	6	2.4
R9	22.9	90/10	67	87	40	6	2.4
R10	24.1	92/8	68	87	40	6	2.4
R11	26.6	90/10	69	90	40	5	1.7

Table S6. Particle size distribution measurement for the research scale MSMPR experiments.

experiment	MSMPR1 X10 after 24h, microns	MSMPR1 X50 after 24h, microns	MSMPR1 X90 after 24h, microns	MSMPR1 X10 after 30h, microns	MSMPR1 X50 after 30h, microns	MSMPR1 X90 after 30h, microns	MSMPR2 X10 after 24h, microns	MSMPR2 X50 after 24h, microns	MSMPR2 X90 after 24h, microns	MSMPR2 X10 after 30h, microns	MSMPR2 X50 after 30h, microns	MSMPR2 X90 after 30h, microns
R3	30.7	91.9	277	29.5	89.9	214.1	35	124.1	383.9	35.6	105.4	252.2
R4	9.5	29.2	304.7	36.5	66.2	121.2	11	32.7	326.6	19.5	47.9	202.9
R5	31.4	70.1	197	44.5	93.3	179.3	26	75.5	229.2	37	86.4	191.5
R6	24.2	170	316.7	24.6	58	277.6	27.1	155	289.4	24.6	148.2	299.6
R7	35.8	290.8	418.6	35.9	86.9	467.3	36.5	259	422.1	31.2	72.8	403.4
R8	35.7	227.1	436.6	31.5	75.8	309.4	33.81	204.2	401.6	31.2	81.7	345.5
R9	31.7	100.4	433.5	nd	nd	nd	30.8	68	343.3	nd	nd	nd
R10	42.5	94.5	397.9	38.7	85.7	360.8	35	77.4	340.2	34.4	75.1	333.9
R11	49.1	100.7	386.2	69.6	151.4	282.6	44.7	103.2	408.1	58.1	138.2	274.4

Exploratory analysis using R[®]/ggplot2[®] looked at univariate trends between PSD and process parameters in Table S6. Correlation does not imply causation at a mechanistic level. MSMPR1 and MSMPR2 τ were left out of the analysis since they are highly correlated with ACN vol% for MSMPR1 and MSMPR2. THF/Water v/v was not included because of its small variation between experiments. Experiment R12 results were left out because the data for the 30 h samples were not available.

Evaluation of the 24 h and 30 h timepoints across most of the experiments shows that the particle size was continuing to evolve, consistent with the crystallization model results. Nevertheless, the statistical analysis was done with the available data. The analysis results show positive correlations with the x10 and the API feed wt% and the x90 vs MSMPR1 temperature. Negative correlations are observed with the x10 and x90 vs ACN vol% in MSMPR1 for both 24 h and 30 h samples. This is consistent mechanistically – lower temperatures in MSMPR1 decrease solubility, and should increase secondary nucleation, while growth rates increase with increasing temperature resulting in a higher x90. Higher antisolvent levels in MSMPR1 should also drive secondary nucleation and result in a larger fraction of small particles. None of these were very strong correlations.

Figure S12 shows univariate trends between MSMPR1 PSD and process parameters. The blue lines in the plots are linear fits and the shaded areas are uncertainty regions of linear fit. Since volpct_ACN_MSMPR2 parameter occurs in operation after MSMPR1, any correlation with it is definitely not causal. Other factors that appear to have some correlation in both 24h and 30h samples are x10 vs API feed wt%, x90 vs MSMPR1 Temp, x90 vs ACN vol% (MSMPR1).

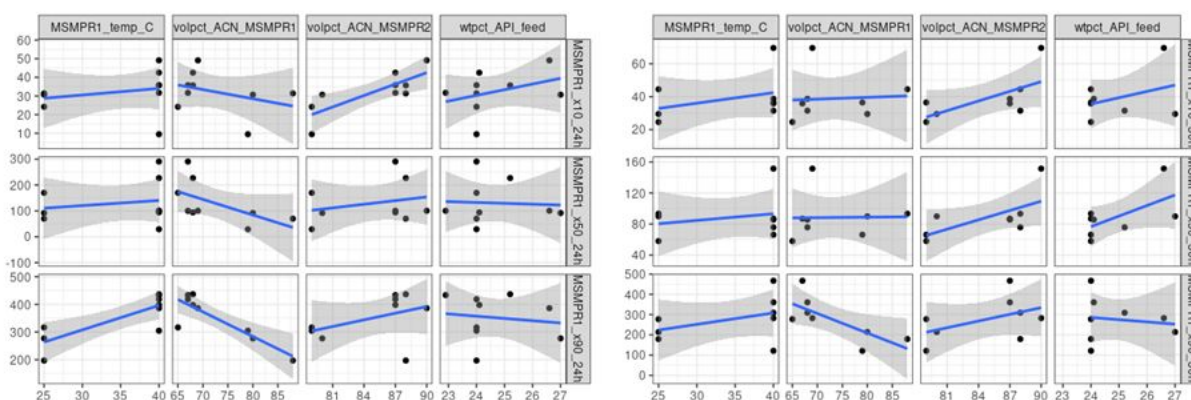


Figure S12. Univariate Trends between MSMPR1 PSD and Process Parameters: 24h PSD vs process parameters on the left. 30h PSD vs process parameters on the right.

Likewise, Figure S13 shows univariate trends between MSMPR2 PSD and process parameters. Factors that appear to have some correlation in both 24h and 30h samples are x10 vs API feed wt%, x10 vs ACN vol % (MSMPR), x90 vs ACN vol% (MSMPR1).

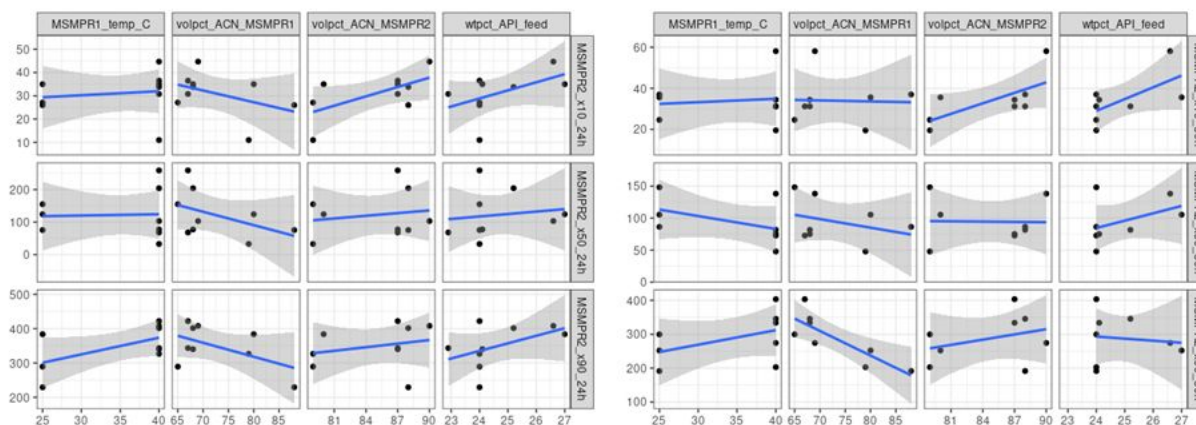


Figure S13. Univariate Trends between MSMPR2 PSD and Process Parameters.

4.b. Supersaturation

Exploratory analysis using R/ggplot2 also looked at univariate trends between supersaturation and process parameters, using the data in Table S7.

Table S7. Supersaturation for research scale MSMPR experiments.

experiment	wt% API in the feed	target feed solvents THF/water v/v	API solution feed rate (mL/min)	continuous experiment duration (h)	# MSMPRs	vol% ACN in solvents in MSMPR1	vol% ACN in solvents in MSMPR2	vol% ACN in MSMPR3	MSMPR1 temp, °C	MSMPR2 temp, °C	MSMPR3 temp, °C	MSMPR1 τ , h	MSMPR2 τ , h	MSMPR3 τ , h	supersaturation in MSMPR1	supersaturation in MSMPR2	supersaturation in MSMPR3
R1	27.6	90/10	0.33	<12	2	80	80	NA	50	10	NA	2	2	NA	nd	nd	NA
R2	26.8	90/10	0.3	11	2	80	80	NA	50	10	NA	2	2	NA	nd	nd	NA
R3	27	90/10	0.125	48	2	80	80	NA	25	10	NA	4	4	NA	31.7	11.9	NA
R4	24	90/10	0.127	30	2	79	79	NA	40	10	NA	4	4	NA	8.78	44.7	NA
R5	24	90/10	0.108	30	2	88	88	NA	25	10	NA	2.6	2.6	NA	56.4	32.9	NA
R6	24	90/10	0.117	30	2	65	79	NA	25	10	NA	6.4	4	NA	3.19	20.1	NA
R7	24	90/10	0.124	30	2	67	87	NA	40	10	NA	6	2.4	NA	5.84	37.3	NA
R8	25.2	89/11	0.129	30	2	68	88	NA	40	10	NA	6	2.4	NA	9.79	24.5	NA
R9	22.9	90/10	0.126	26	2	67	87	NA	40	10	NA	6	2.4	NA	-0.1	35.5	NA
R10	24.1	92/8	0.133	26	2	68	87	NA	40	10	NA	6	2.4	NA	15.5	69.6	NA
R11	26.6	90/10	0.11	67	2	69	90	NA	40	10	NA	5	1.7	NA	1.61	14.2	NA
R12	25.6	90/10	0.12	30	2	69	90	NA	50	25	NA	5	1.7	NA	-19	11.2	NA
R13	26.6	90/10	0.124	12	2	69	90	NA	50	10	NA	5	1.7	NA	-29	15.6	NA
R14	27.5	90/10	0.123	32	3	69	92	92	50	25	10	5	1.7	1.7	-21	4.78	6.89
R15	25.1	90/10	0.229	30	3	73	86	86	50	40	10	5.3	3.1	3.1	12.3	17.3	32.9
R16	25.1	90/10	0.229	30	3	73	88	88	50	40	10	5.3	2.7	2.7	10	15.8	33.7

R17	25.1	90/10	0.225	30	3	73	83	83	50	40	10	5.3	3.5	3.5	7.99	0.59	20.8
-----	------	-------	-------	----	---	----	----	----	----	----	----	-----	-----	-----	------	------	------

As expected, supersaturation in MSMPR1 decreased with higher temperature, longer τ , and lower ACN antisolvent in MSMPR1 (Figure S14). In the data analysis, the incremental impact of τ was lower since it had high correlation with ACN vol% in MSMPR1.

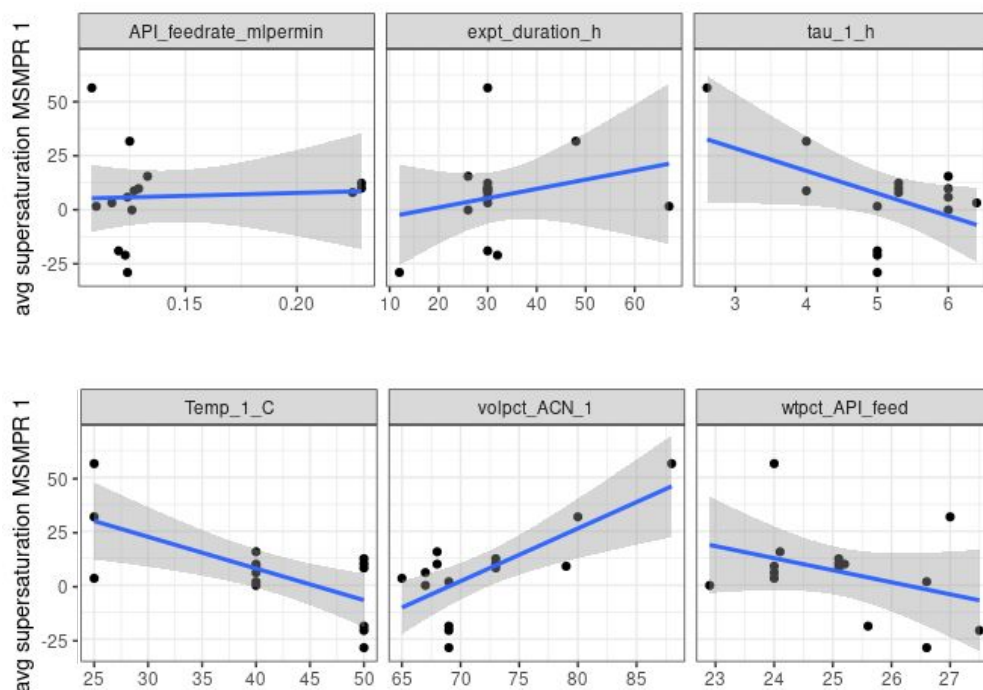


Figure S14. Impact of τ , temperature, volume % ACN antisolvent, wt% API in the feed, API feed rate, and experiment duration on supersaturation in MSMPR1

The correlation of MSMPR1 supersaturation with process variables is listed below.

	avg_super saturation (MSMPR1)
wtpct_API_feed	-36%
API_feedrate_mlpermin	6%
expt_duration_h	25%
volpct_ACN_1	73%
Temp_1_C	-67%
tau_1_h	-50%

MSMPR1 supersaturation shows correlation ($\geq 50\%$) with the following parameters.

- ACN vol % in MSMPR1 (positive)
- MSMPR1 Temp (negative)

- MSMPR1 tau (negative)
 - The incremental impact of tau is lower since it has high correlation with ACN vol% in MSMPR1 (-93%)

Doing a forward stepwise regression also picked the same variables.

Also expected, supersaturation decreased with higher temperature in MSMPR2 as well. It also correlated to wt% API in the feed material, but this is suspicious because variation in feed level is narrow (23%-27%).

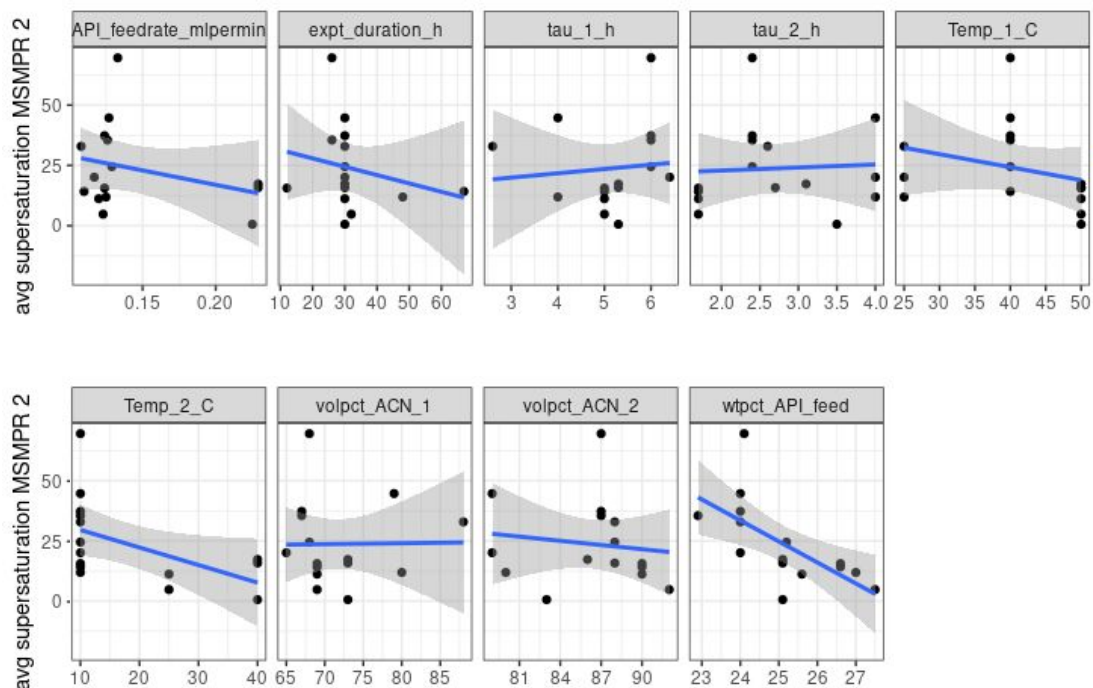


Figure S15. Correlation of MSMPR 2 supersaturation with process variables.

The correlation of MSMPR 2 supersaturation with process variables is listed below.

	avg_super saturation (MSMPR2)
wtpct_API_feed	-65%
API_feedrate_mlpermin	-30%
expt_duration_h	-23%
volpct_ACN_1	1%
volpct_ACN_2	-14%
Temp_1_C	-29%
Temp_2_C	-51%
tau_1_h	10%
tau_2_h	6%

MSMPR2 supersaturation shows correlation ($\geq 50\%$) with

- Wt% API in feed (negative) (though the actual variation in feed level is narrow 23%-27%)

- MSMPR2 Temp (negative)

Doing a forward stepwise regression also picked the same variables.

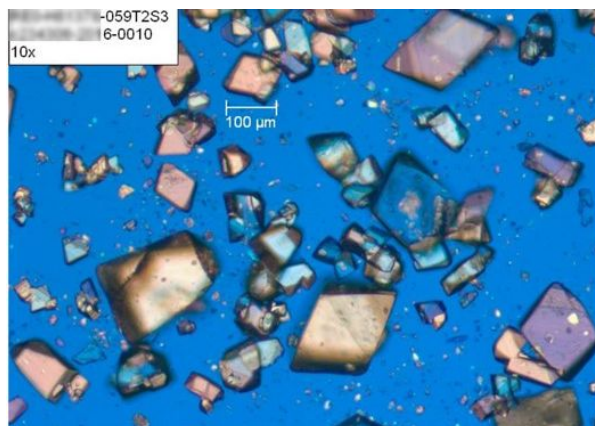
Correlation within Process Parameters.

xvar	wtpct_API_feed	API_feedrate_mlin	expt_duration_h	volpct_ACN_1	volpct_ACN_2	Temp_1_C	Temp_2_C	tau_1_h	tau_2_h
wtpct_API_feed	100%	-2%	36%	0%	34%	27%	18%	-21%	-31%
API_feedrate_mlin	-2%	100%	-16%	5%	-9%	53%	90%	16%	26%
expt_duration_h	36%	-16%	100%	12%	-5%	-29%	-10%	-18%	4%
volpct_ACN_1	0%	5%	12%	100%	-26%	-38%	2%	-93%	37%
volpct_ACN_2	34%	-9%	-5%	-26%	100%	53%	12%	5%	-97%
Temp_1_C	27%	53%	-29%	-38%	53%	100%	65%	28%	-49%
Temp_2_C	18%	90%	-10%	2%	12%	65%	100%	7%	5%
tau_1_h	-21%	16%	-18%	-93%	5%	28%	7%	100%	-11%
tau_2_h	-31%	26%	4%	37%	-97%	-49%	5%	-11%	100%

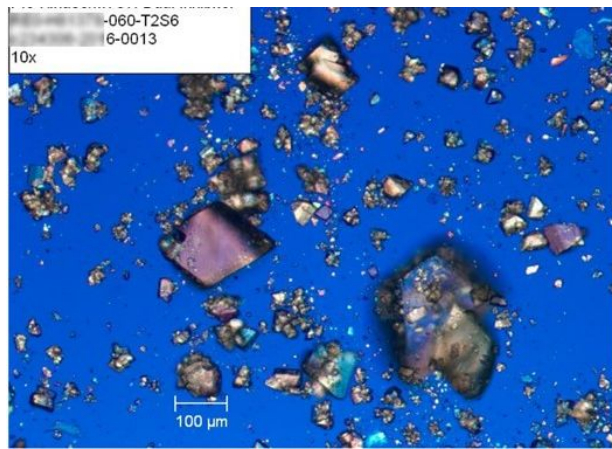
5. Microscopy

5.a. Research scale crystallizations

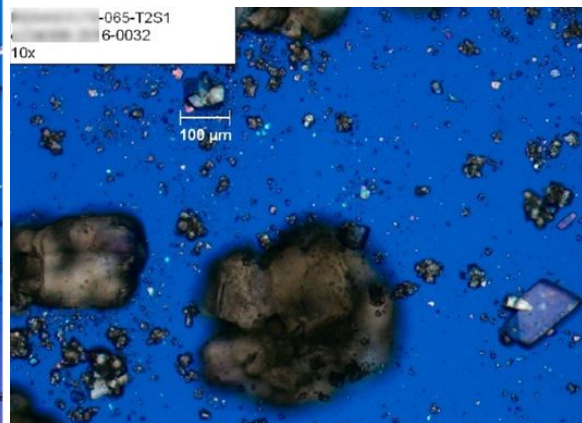
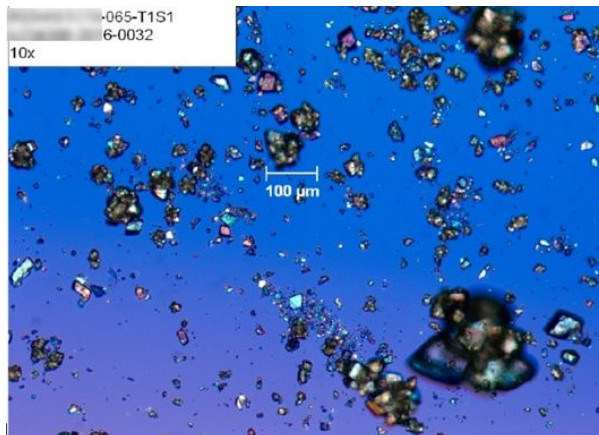
Experiment R1 (8 h of flow) shown below. Less agglomeration, more single crystals, some fines, but they do not look agglomerated. Could be some attrition from agitation.



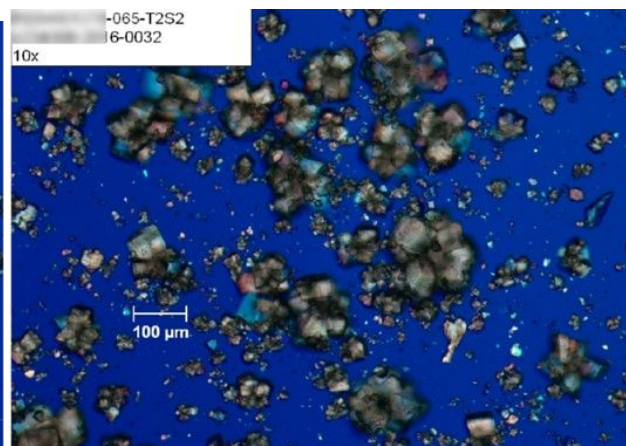
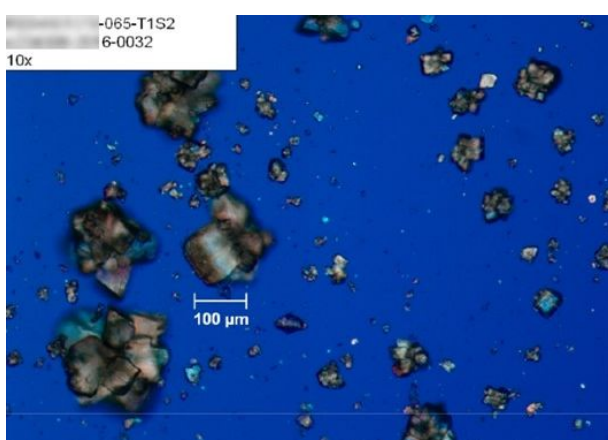
Experiment R2 research scale (10.5 h of flow) shown below. The small crystals look like primarily agglomerates. Even the large crystals look like mainly agglomerates.



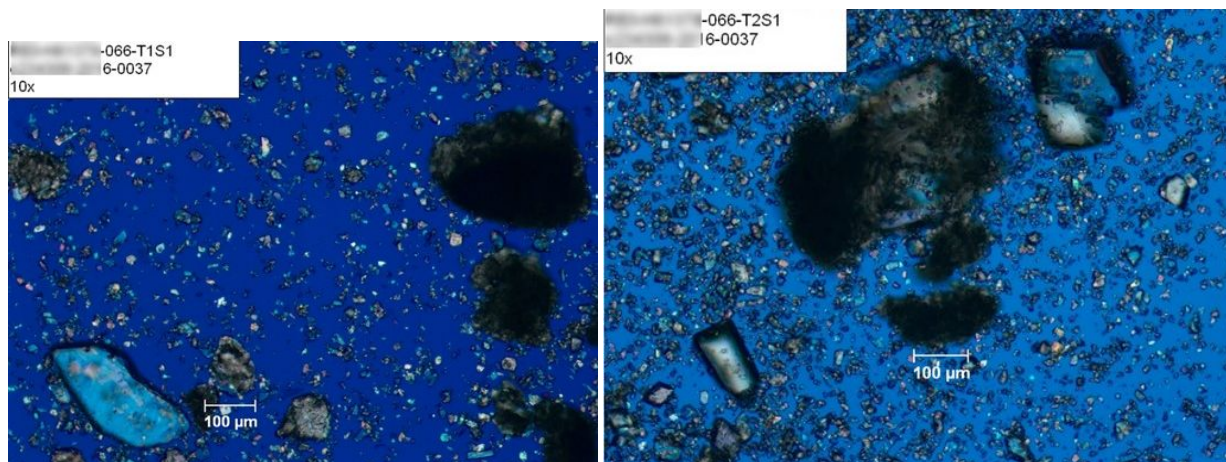
Experiment R3 research scale (24 h) shown below. MSMPR1 on the left and MSMPR2 on the right. Look like mainly agglomerates.



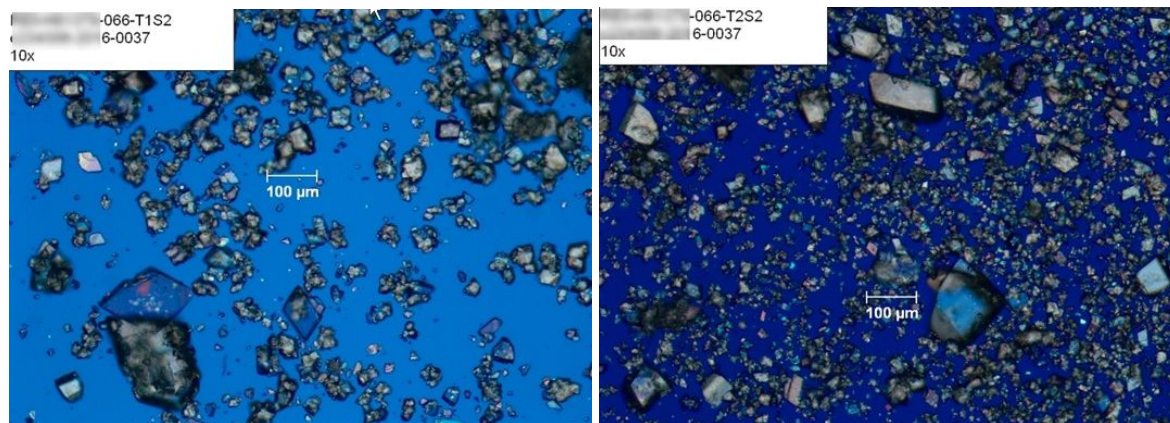
Experiment R3 research scale (30 h) shown below. MSMPR1 on the left and MSMPR2 on the right. Very few single crystals, mostly agglomerates. There are a larger number of fines in the second MSMPR.



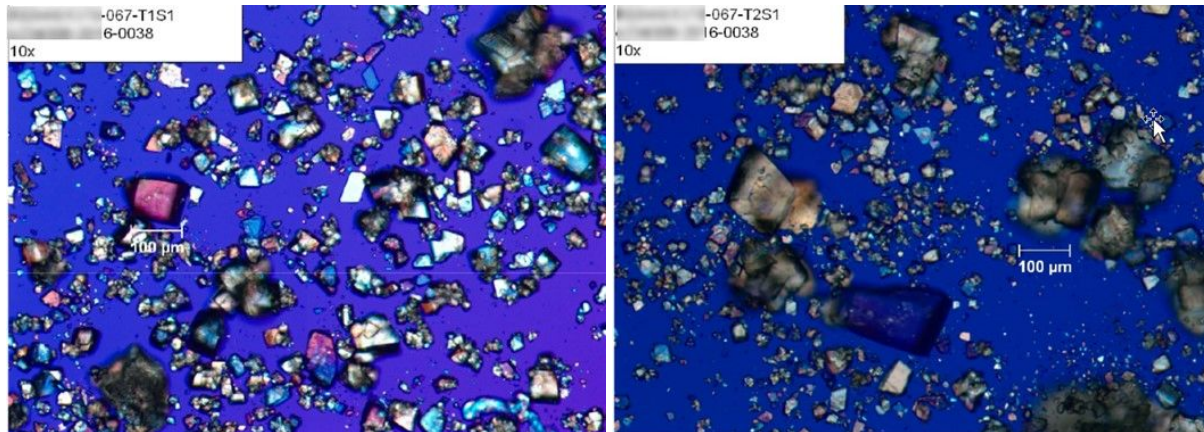
Experiment R4 research scale (24 h) shown below. MSMPR1 on the left and MSMPR2 on the right. A lot more fines, not agglomerated. The larger particles are not well defined. Nucleation looks high during this experiment. All the antisolvent was added in the first MSMPR. May have high secondary nucleation or attrition in the second MSMPR because of the larger number of fines. The smaller particles that are not agglomerates are most likely nucleation.



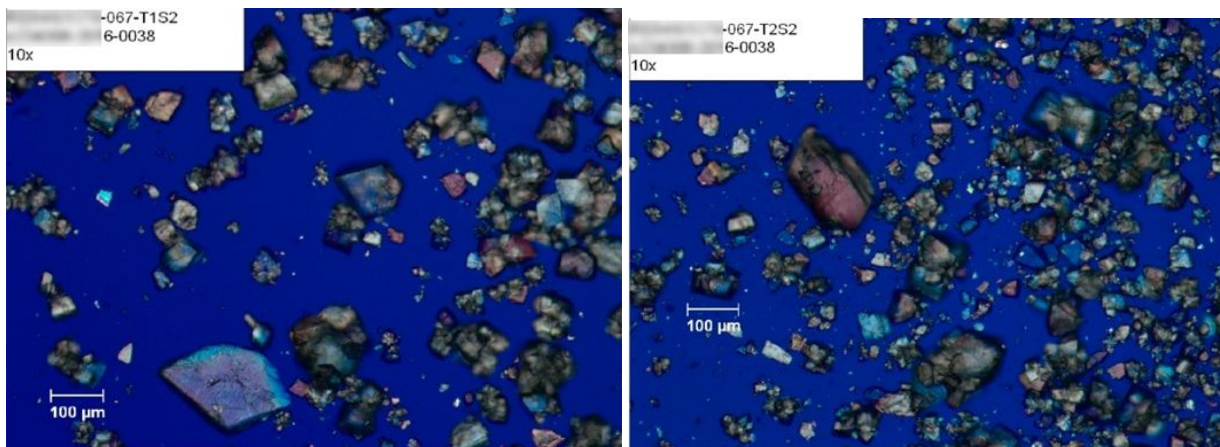
Experiment R4 research scale (30 h) shown below. MSMPR1 on the left and MSMPR2 on the right. There are a larger number of fines in the second MSMPR. The smaller particles that are not agglomerates are most likely nucleation.



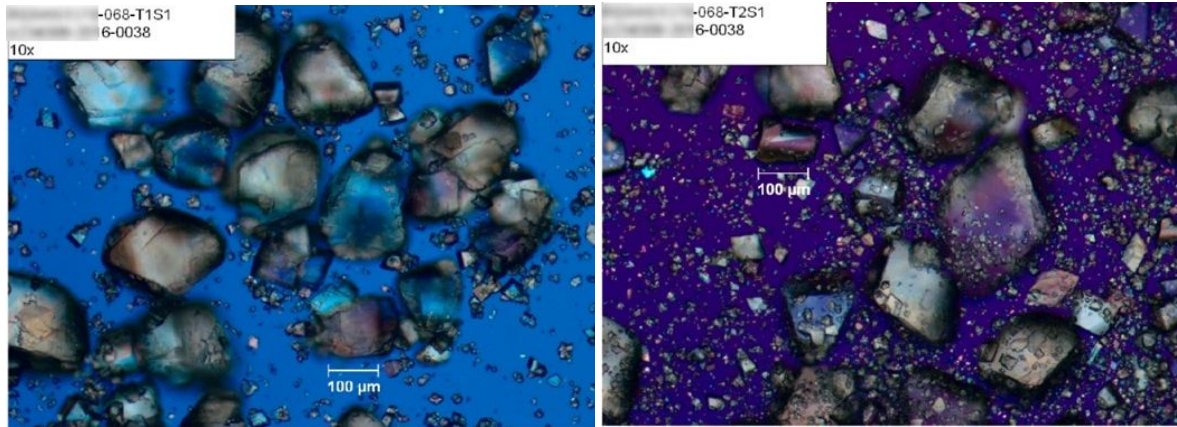
Experiment R5 research scale (24 h) shown below. MSMPR1 on the left and MSMPR2 on the right. Some agglomerates, but mostly individual crystals. The larger particles in the image on the right (MSMPR2) look like agglomerates.



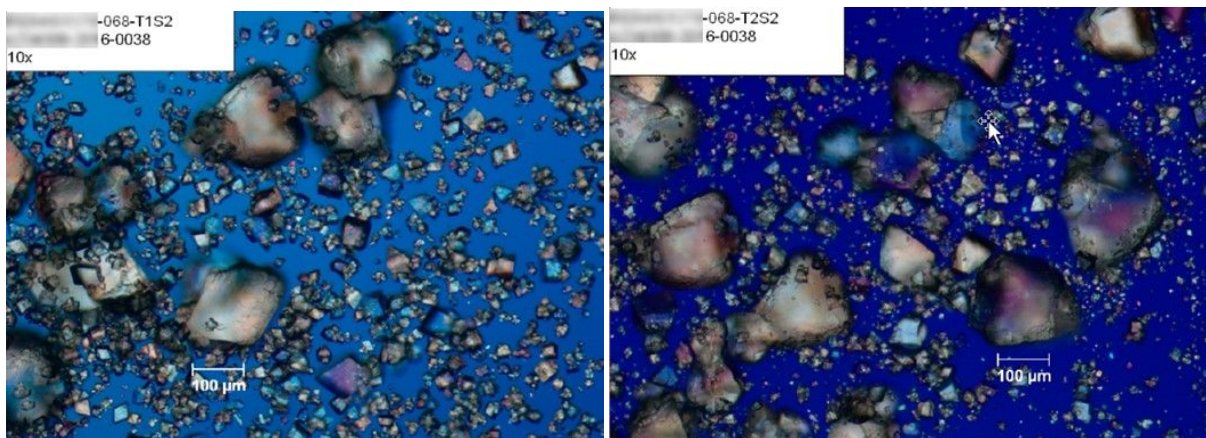
Experiment R5 research scale (30 h) shown below. MSMPR1 on the left and MSMPR2 on the right. More agglomerates in MSMPR1 compared to the 24h sample.



Experiment R6 research scale (24 h) shown below. MSMPR1 on the left and MSMPR2 on the right. Much bigger particles than in the Experiment R5 images. The larger particles are less agglomerated. These are larger single crystals but the edges do not look sharp. Also more small fines in MSMPR2 compared to the Experiment R5 images. The fines appear less agglomerated.



Experiment R6 research scale (30 h) shown below. MSMPR1 on the left and MSMPR2 on the right.

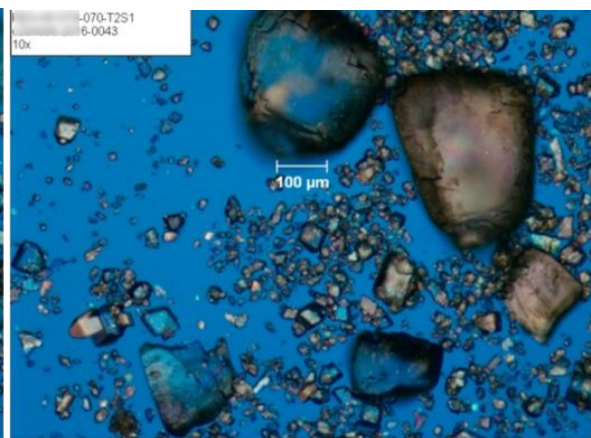
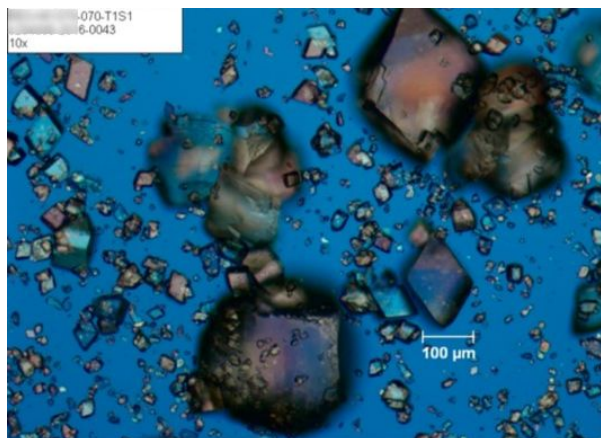


Process conditions for experiments R7 – R12 research scale were all near representative baseline conditions for 2 MSMPRs in series.

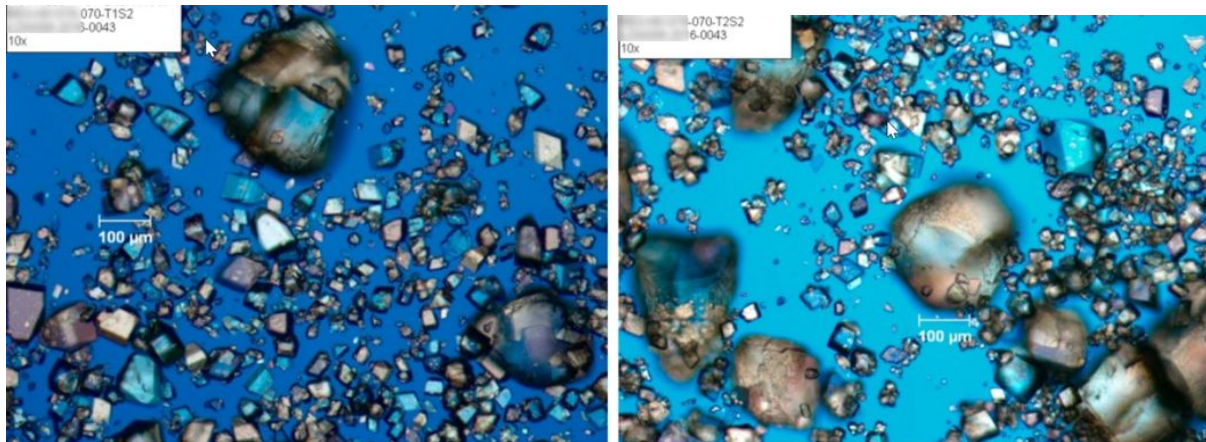
Experiment R7 research scale Isolated solids from filter shown below. Some single larger crystals that look rhombohedral with sharper edges. There is a small amount of agglomeration, for example there is one in the middle that looks like it may be growing in two different directions. The agglomerates primarily look to be the smaller particles, which may have been forming in MSMPR2.



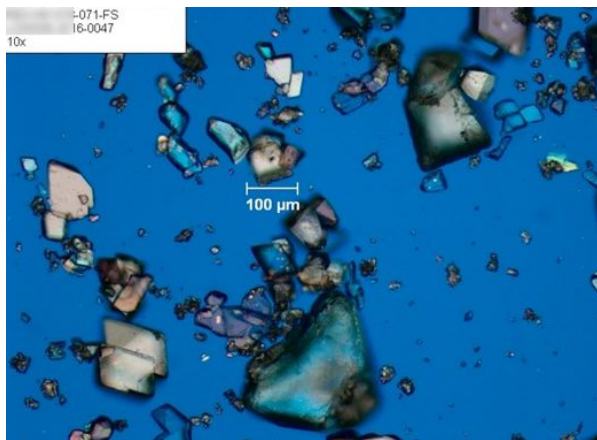
Experiment R8 research scale (24 h) shown below. MSMPR1 on the left and MSMPR2 on the right. The Experiment R8 images show most the characteristics seen among these images across the various experiments. They contain some large individual nicely faceted rhombohedral crystals, some large agglomerates that look rounded by attrition, small individual crystals that are rhombohedral, and also small agglomerates. The small crystals look individual for the most part, fairly uniform and they are nicely shaped. Some large crystals, but still see the fines.



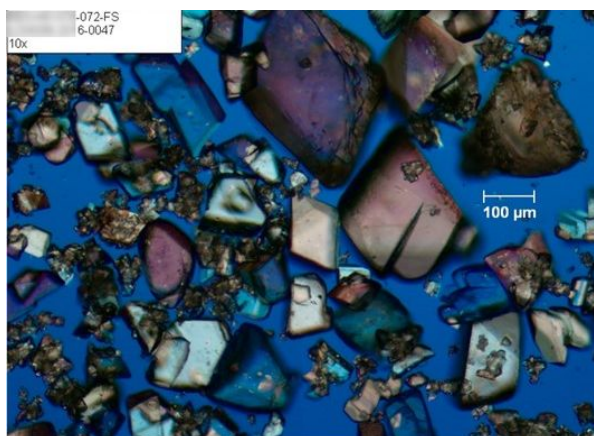
Experiment R8 research scale (30 h) shown below. MSMPR1 on the left and MSMPR2 on the right.



Experiment R9 research scale Isolated Solids shown below.

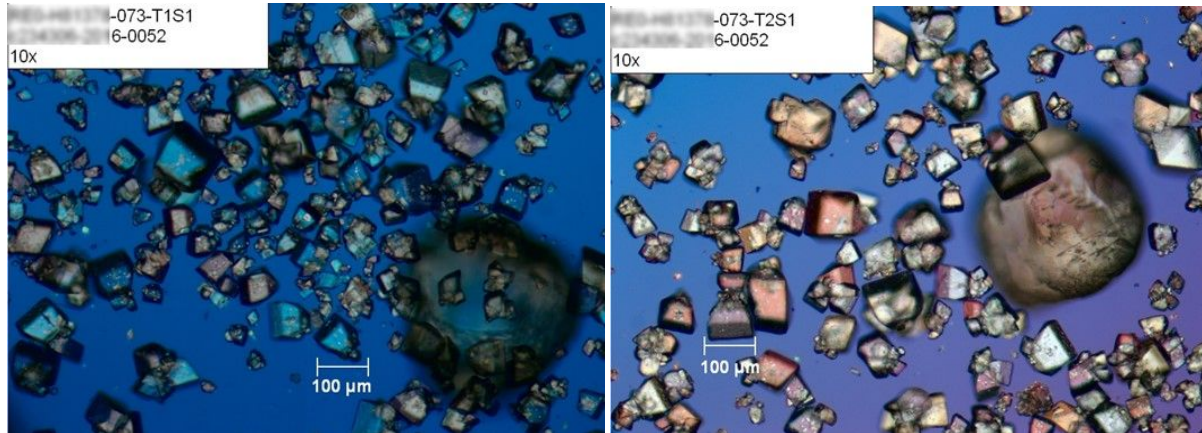


Experiment R10 research scale Isolated Solids shown below. Larger particles and fewer fines.

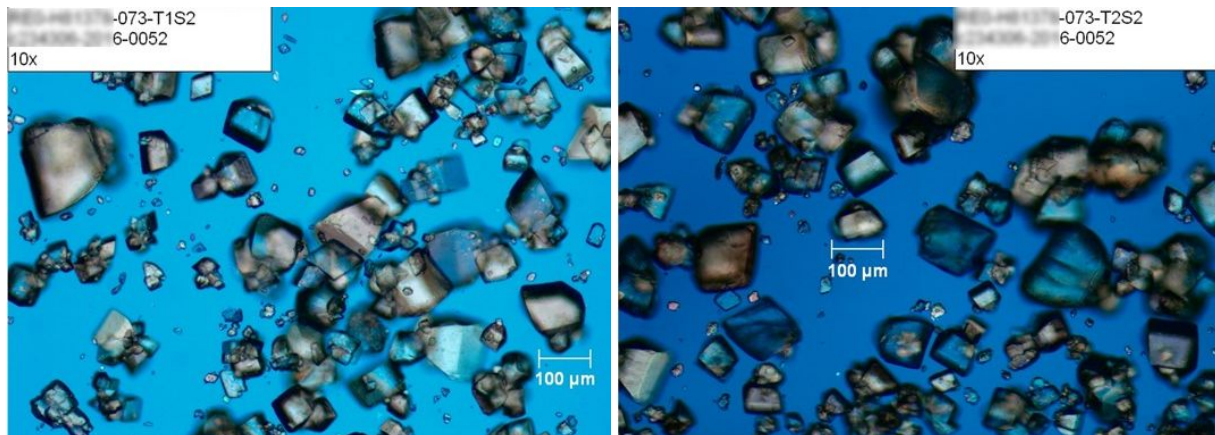


Experiment R11 research scale (24 h) shown below. MSMPR1 on the left and MSMPR2 on the right. Experiment R11 has mostly nice uniform individual crystals, and you can see the rhombohedral shapes and images. The edges for most of the crystals are sharper and defined. The very large particles at the

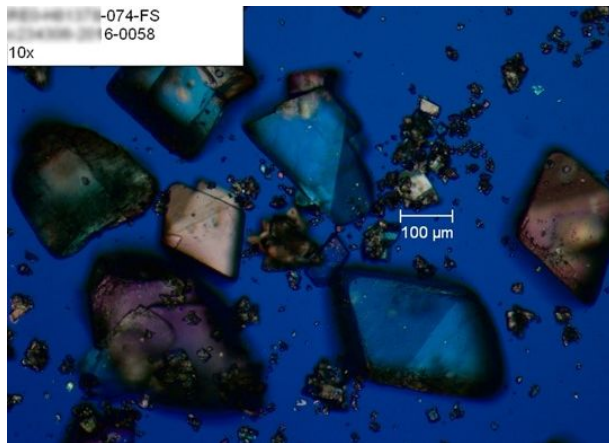
24 hour time point, on the other hand, look like they might've been retained in the crystallizers for an extended period of time beyond the typical τ , causing the edges to suffer attrition. They may be large individual crystals that attritted. It is certainly plausible that the large particles spend longer time in the crystallizers than the small particles. There are some hints of agglomeration but not many. It is difficult to say whether the small particles attritted pieces or if they are secondary nucleation. Some of the smaller particles look like groups of agglomerates.



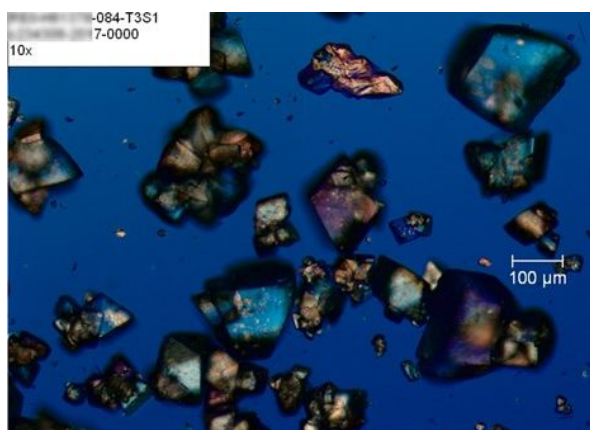
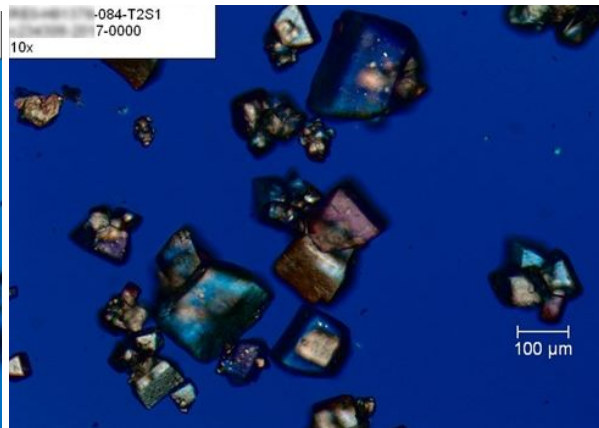
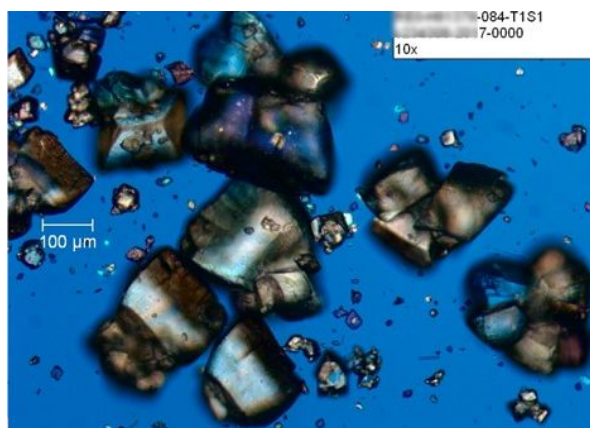
Experiment R11 research scale (30 h) shown below. MSMPR1 on the left and MSMPR2 on the right.



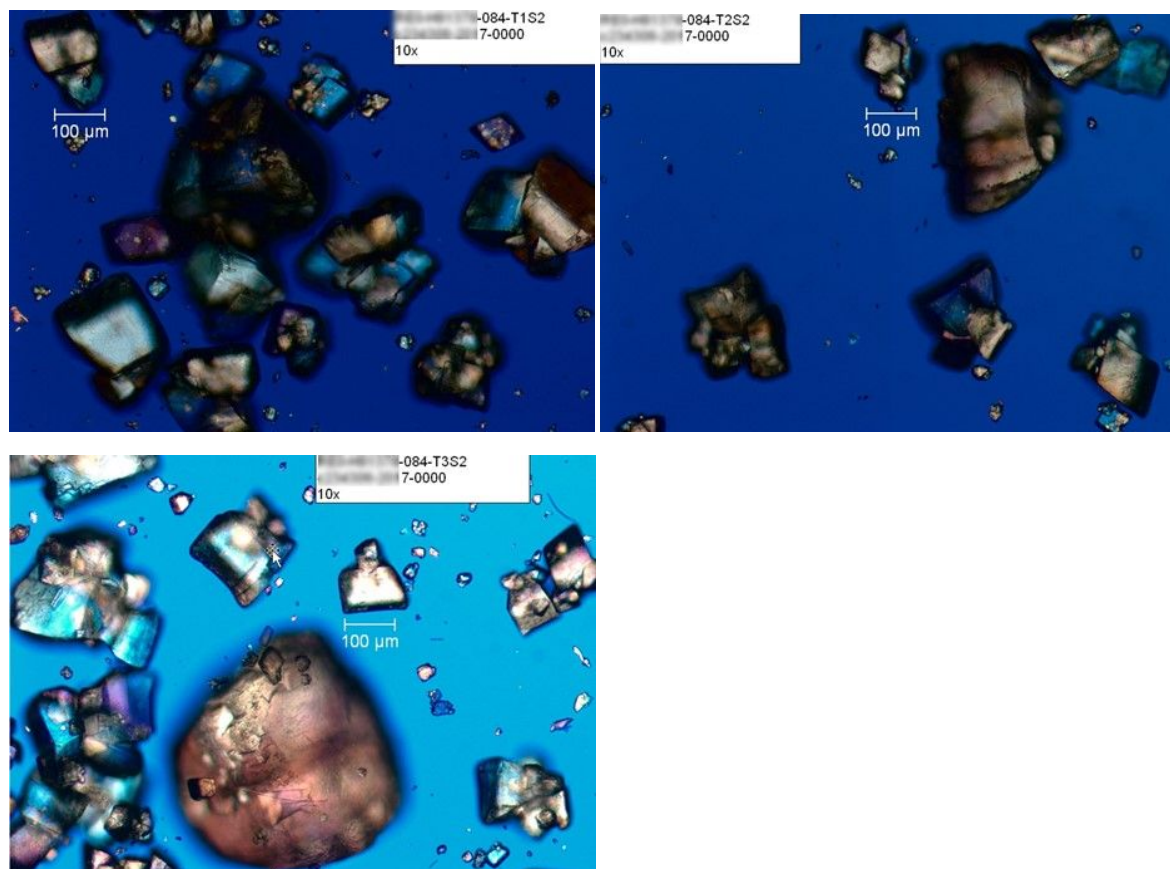
Experiment R12 research scale Isolated Solid shown below. Some very large individual well defined crystals, and some fines that look agglomerated.



Experiment R14 research scale (24 h) shown below. MSMPR1 on the left and MSMPR2 on the right, and MSMPR3 at the bottom. Better angles and edges on the larger crystals. MSMPR3 had agglomerates. Does not look like a lot of small particles or smaller agglomerates.



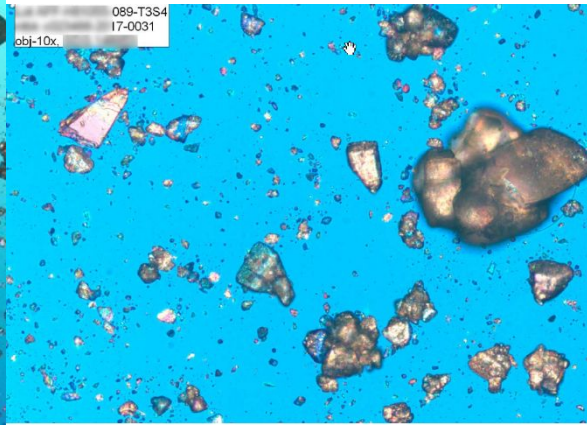
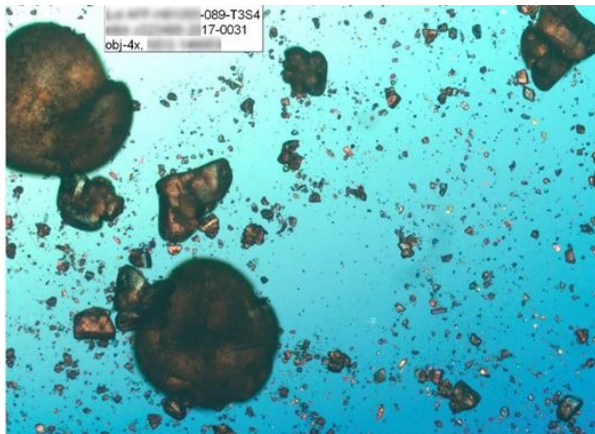
Experiment R14 research scale (30 h) shown below. MSMPR1 on the left and MSMPR2 on the right, and MSMPR3 at the bottom.



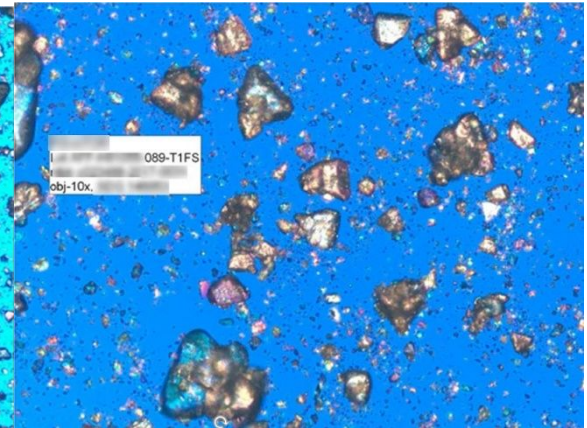
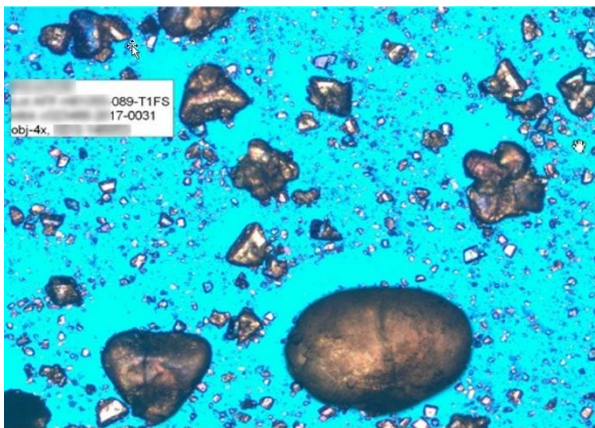
5.b. Pilot scale crystallizations

Experiment P4 shown below. The spherical looking particles are unusual. We are not exactly sure what might be causing it. They look like spheres or eggs. The spherical nature is puzzling. It looks like a larger number of fines in MSMPR3 compared to MSMPR1 and 2. It looks like a bimodal particle size, large agglomerates or spheres and then a bunch of fines, supported by the observation that the Malvern PSDs are not a gaussian distribution.

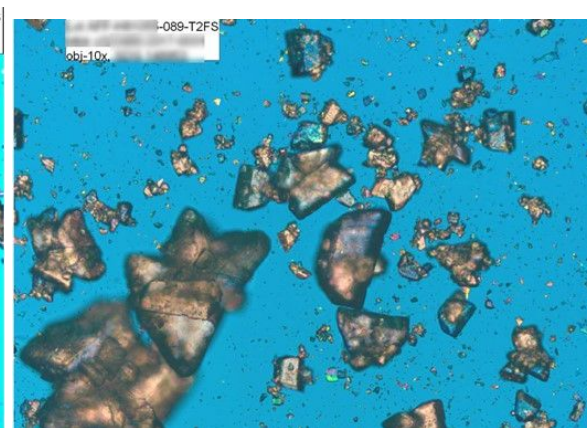
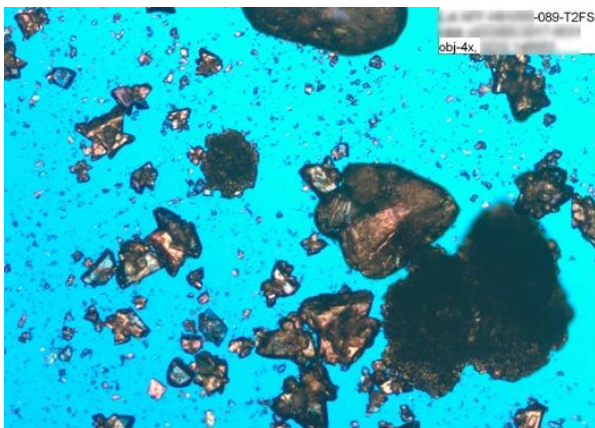
MSMPR3 crystal images shown below.



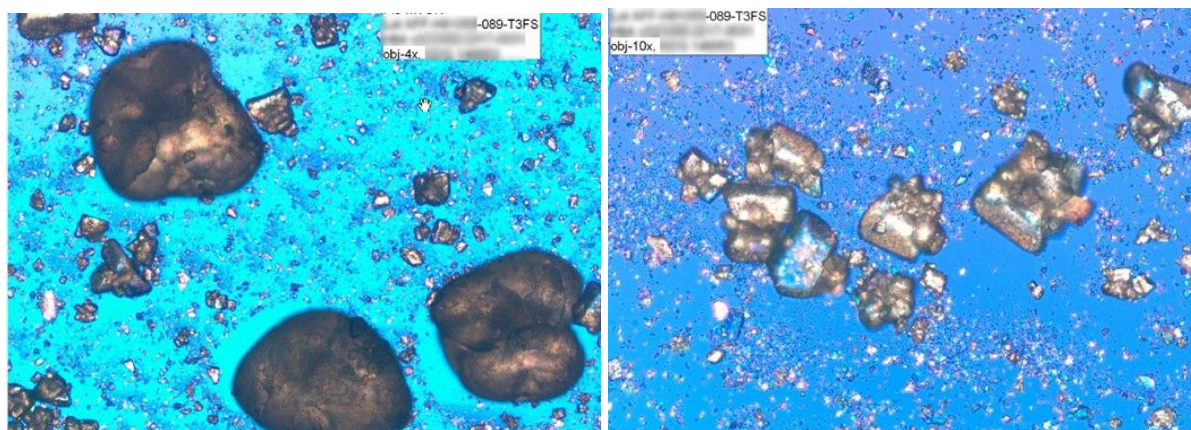
MSMPR1 crystal images shown below.



MSMPR2 crystal images shown below.



MSMPR3 crystal images shown below.



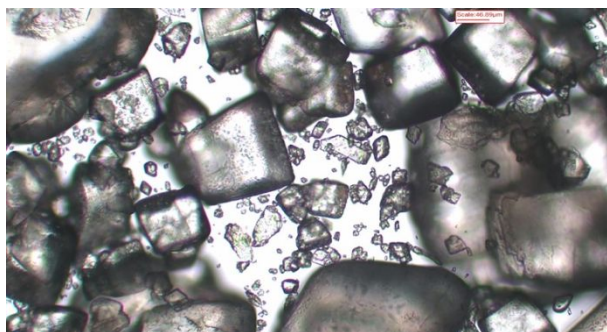
5.c. Manufacturing scale crystallizations

Batches 1-6 were generated before Christmas break, when the manufacturing plant experienced many more stoppages and holds. It is not surprising if particle size and microscopic images vary among those batches. Process holds longer than 4 h were subjected to a thermocycle before restarting. All 3 crystallizers were heated to 60°C for 1 h and then cooled back down to operating temperatures when the flows restarted. This would have impacted the particle size distribution in those scenarios. This happened 9 times during the first 6 batches and then only 2 times during batches 8 through 15. The process was much steadier during batches 8 through 15. Some images show more fines than others, for example batches 10, 12, and 14, and some show more large agglomerates, and that was partially due to the selection of the analyst.

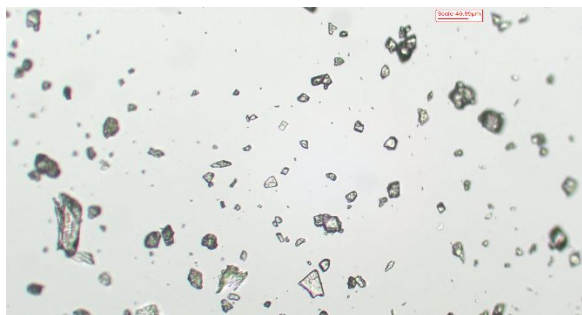
cGMP Manufacturing Batch 4 shown below.



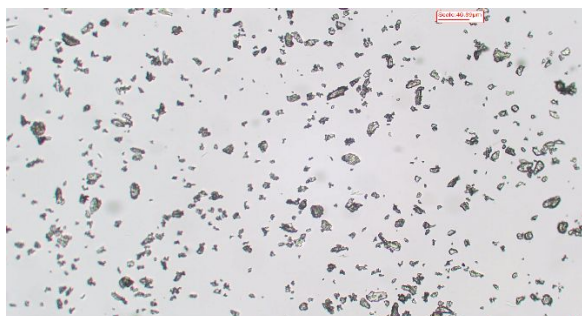
cGMP Manufacturing Batch 5 shown below. The microscopy shows several individual crystals that are large. They have a similar rhombohedral shape as what was seen for the research scale runs. There is some breakage, there are some irregular crystals and some fines, but for the most part the crystals look very good with not as much agglomeration. Batches 4 and 5 look a lot different, although the psd results for x10, x50, and x90 in Table S4 would not indicate that they would be so different. Batch 4 looks like it has more fines, and batch 5 looks like it has more large well-defined crystals. It might be because of the personal choice of the analyst if they were searching around and selecting which section of the slide to take the picture.



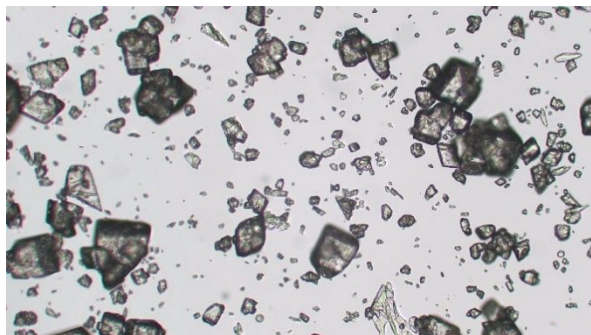
cGMP Manufacturing Batch 6 shown below.



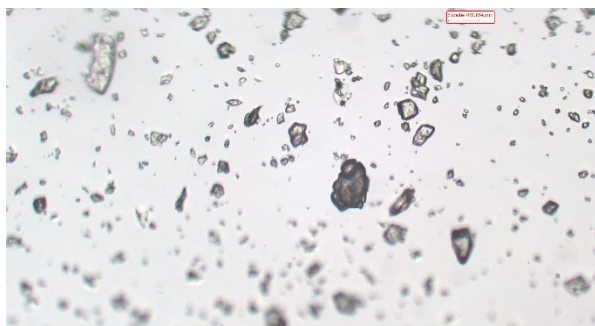
cGMP Manufacturing Batch 7 shown below.



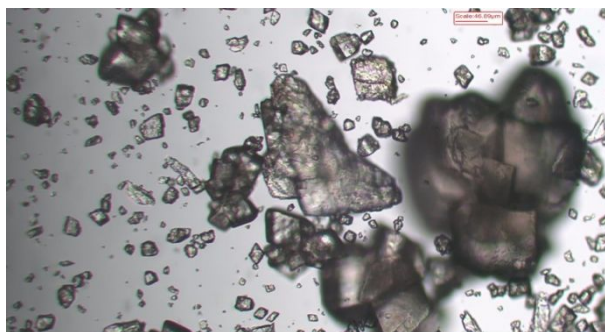
cGMP Manufacturing Batch 8 shown below.



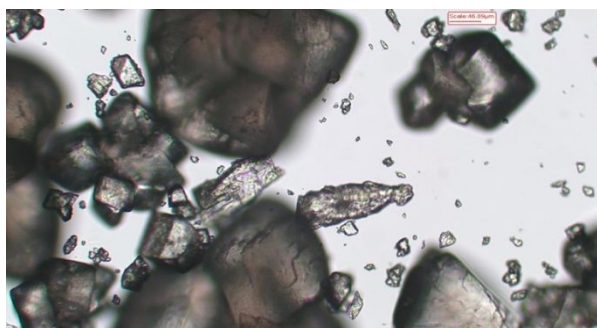
cGMP Manufacturing Batch 9 shown below.



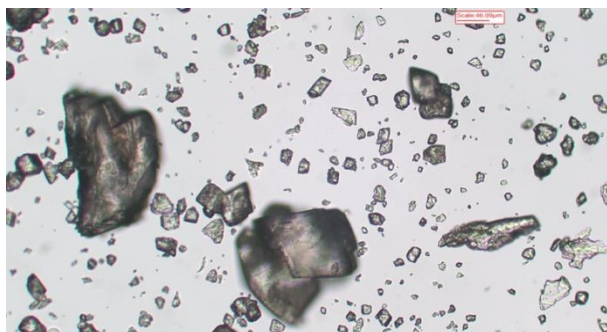
cGMP Manufacturing Batch 10 shown below. Batch 10 for the manufacturing scale looks a lot different than batch 5. It shows less individual rhombohedral type crystals, more agglomerates, a larger number of fines, and the large particle that is partly in focus looks like an agglomerate. x10, x50, x90 data in the main paper would not lead us to think that the images would be so different for the different batches, but again it may just be a difference in where the analyst decided to take the picture.



cGMP Manufacturing Batch 11 shown below.



cGMP Manufacturing Batch 12 shown below. Large agglomerates, and the fines look like single crystals.



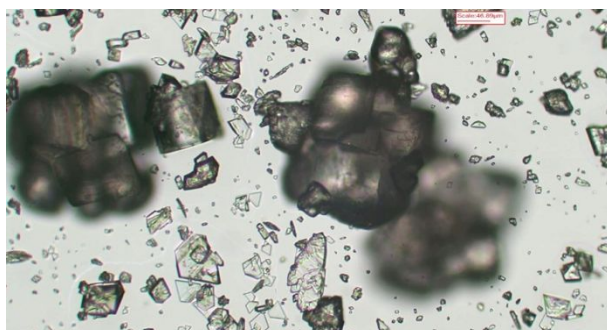
cGMP Manufacturing Batch 13 shown below. Some of the batches appear to have a larger number of fines, like batches 12, 13, and 14. Batch 13 has some nice regular crystals in it as well.



cGMP Manufacturing Batch 14 shown below. Batch 14 looks like it has a lot more fines in it. From the x10, x50, and x90 data given in Table S4 we would guess that batch 13 would have more fines than batch 14, but the images make it look like it is the other way around. Therefore, the images are not taken to represent the entire batch. Looking at the multiple images gives an overall idea of the crystals.




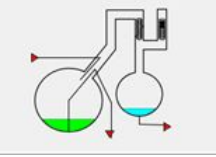
cGMP Manufacturing Batch 15 shown below.

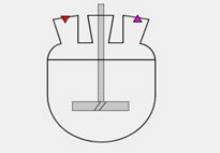


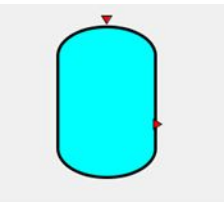
6. RTD Model Equations

A summary of the RTD model elements, assumptions, and the corresponding equations is presented in Table S8.

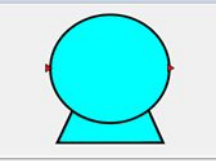


Table S8. RTD model elements and equations

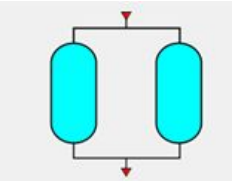
Element	Scheme	Assumptions	Equations
Feed		-Feed composition is known	$w_{feed,j} = w_j$ Components and corresponding molecular weights need to be defined.
Evaporator		<ul style="list-style-type: none"> - Continuous distillation - The fraction of component mass that goes to the bottoms is known (experimentally determined correlation for THF and water) - Evaporator content operates as a CSTR - Constant mass in continuous equipment - Flow rate of the distillate is determined by a pump - Single input, two outputs - Only THF and Water are distilled 	$m_{distillate} = Rm_t$ $m_{bottoms} = (1 - R)m_t$ $R = 0.9 - w_{distillate,water}$ $F_{bottoms} = (F_{feed} + F_{additional}) - F_{distillate}$ $w_{distillate,i} = \frac{m_{d,i}}{m_{distillate}}$ $w_{bottoms,i} = \frac{m_{b,i}}{m_{bottoms}}$ $m_{bottoms} \frac{dw_{bottoms,i}}{dt} = F_{feed}w_{feed,i} + F_{additional}w_{additional,i} - F_{distillate}w_{distillate,i} - F_{bottoms}w_{bottoms,i}$ $w_{distillate,THF} = 1 - w_{distillate,water}$ $w_{distillate,i \neq THF,water} = 0$ $if w_{bottoms,water} \geq w_{water,max}$ $w_{distillate,water} = Slope * w_{water,max} + Intercept$ Else $w_{distillate,water} = Slope * w_{bottoms,water} + Intercept$ $m_i = m_{d,i} + m_{b,i}$

			<p>With:</p> <p>F_{feed} = feed charge mass flowrate, Kg/s</p> <p>$F_{\text{distillate}}$ = Distillate discharge mass flowrate, Kg/s</p> <p>$w_{\text{feed},i}$ = weight fraction of species i in feed stream, Kg/Kg</p> <p>$F_{\text{additional}}$ = additional feed stream , Kg/s</p> <p>$w_{\text{additional},i}$ = weight fraction of species i in additional feed stream, Kg/Kg</p> <p>$w_{\text{initial},i}$ = weight fraction of species i at $t = 0$, Kg/Kg</p> <p><i>Slope</i> : slope of the water distribution coefficient, dimensionless;</p> <p><i>Intercept</i> : Intercept of the linear relationship for the water distribution coefficient, Kg/Kg</p> <p>$w_{\text{water,max}}$ = maximum amount of water in bottoms above which distillate water content does not increase, Kg/Kg</p> <p>m_t = total mass of material in evaporator, Kg;</p> <p>Components and corresponding molecular weights need to be defined. Defined initial conditions are needed.</p>
MSMPR		<ul style="list-style-type: none"> - Each phase in the MSMPR (solid and liquid) is well-mixed - The fraction of the total component mass going to the solid phase is known - Constant volume - Constant density 	<p>$\rho V = m_t$</p> <p>$F_{\text{in}} = \sum_{i=1}^N F_{\text{feed},i}$</p> <p>$F_{\text{out}} = F_{\text{in}}$</p> <p>$F_{\text{out,solid}} = F_{\text{out}} \frac{m_{\text{solid phase}}}{m_t}$</p> <p>$F_{\text{out,liquid}} = F_{\text{out}} \frac{m_{\text{liquid phase}}}{m_t}$</p> <p>$m_{\text{solid phase}} = \sum_j m_{\text{solid},j} \quad (j = \text{components})$</p>

		<ul style="list-style-type: none"> - Multiple inputs, single output 	<p>With:</p> <p>ρ = density solution, Kg/m³</p> <p>V = Volume, m³</p> <p>$F_{feed,i}$ = Inlet stream i mass flowrate, kg/s</p> <p>$w_{feed\ i,j}$ = weight fraction of component j in inlet stream i, Kg/Kg</p> <p>$w_j^{solid,user\ defined}$ = fraction of mass going to solid phase</p> <p>$m_{liquid\ phase} = \sum_j m_{liquid,j}$ (j=components)</p> <p>$w_{solid,j} = \frac{m_{solid,j}}{m_{solid\ phase}}$</p> <p>$w_{liquid,j} = \frac{m_{liquid,j}}{m_{liquid\ phase}}$</p> <p>$m_{solid,j} = m_j w_j^{solid,user\ defined}$</p> <p>$m_{liquid,j} = m_j (1 - w_j^{solid,user\ defined})$</p> <p>$\frac{dm_j}{dt} = \sum_{i=1}^{n_{feed}} F_{feed,i} * w_{feed\ i,j} - F_{out,solid} w_{solid,j} - F_{out,liquid} w_{liquid,j}$</p> <p>Components and corresponding molecular weights need to be defined. Defined initial conditions are needed.</p>
Product Drum		<ul style="list-style-type: none"> - The vessel's content is treated as a well-mixed volume - Constant density - Multiple inputs, single output - Tank collects inlet streams until the user defined 	<p>$\rho V = m_t$</p> <p>$m_j = w_j m_t$</p> <p>$F_{in} = \sum_{i=1}^N F_{feed,i}$</p> <p>$F_{empty} = 1000 F_{in}$</p> <p>When Drum_Status = "Tank_Fill"</p>

		<p>collection mass is reached.</p> $w_{j,out} = 0$ $F_{out} = 0$ $\frac{dm_t}{dt} = \sum_{i=1}^{n_{feed}} F_{feed,i}$ $\frac{dm_j}{dt} = \sum_{i=1}^{n_{feed}} F_{feed,i} w_{feed,i,j}$ <p>Switch to "Tank_Empty" when $m_t > m_{coll}$</p> <p>When Drum_Status = "Tank_Empty"</p> $w_{j,out} = w_j$ $F_{out} = F_{empty}$ $\frac{dm_t}{dt} = -F_{empty}$ $\frac{dm_j}{dt} = \sum_{i=1}^{n_{feed}} F_{feed,i} w_{feed,i,j} - F_{empty} w_j$ <p>Switch to "Tank_Fill" when $m_t < m_{coll} * 1e^{-8}$</p> <p>Initial Conditions:</p> $m_t = \rho V^o$ $w_j = w_j^o$ <p>With:</p>
--	--	---

			ρ = density solution, Kg/m ³ V^o = Initial volume, m ³ w_j^o = Initial weight fraction of component j , Kg/Kg m_{coll} = Collection mass for the drum, Kg $F_{feed,i}$ = Inlet stream i mass flowrate, kg/s $w_{feed,i,j}$ = weight fraction of component j in inlet stream i , Kg/Kg Components and corresponding molecular weights need to be defined. Defined initial conditions are needed.
Pump		<ul style="list-style-type: none"> - Mass flow rate is known - No material holdup in pump 	$F_{feed} = F_{out}$ $w_i = w_{feed,i}$ With: F_{feed} = flow rate set point, kg/s $w_{feed,i}$ = weight fraction of component i in feed stream, Kg/Kg Components and corresponding molecular weights need to be defined.
Sink		This model element is only used to complete flowsheets.	Mass fraction of components and mass flow rate from the inlet stream are stored
Filter		<ul style="list-style-type: none"> - Phases in the filter (i.e., liquid and solid) are individually well-mixed - Constant volume of phases in the filter 	$\rho_{solid} V_{solid} = m_{solid\ phase}$ $\rho_{liquid} V_{liquid} = m_{liquid\ phase}$ $F_{in,solid} = F_{feed,solid}$ $F_{in,liquid} = F_{feed,liquid}$ $F_{in,solid} = F_{out,solid}$ $F_{in,liquid} = F_{out,liquid}$ $m_{solid\ phase} w_{solid,j} = m_{solid,j}$ $m_{liquid\ phase} w_{liquid,j} = m_{liquid,j}$

		<ul style="list-style-type: none"> - Constant density of phases - Single input, two outputs 	$\frac{dm_{solid,j}}{dt} = F_{feed,solid} * w_{feed i,solid} - F_{out,solid} w_{solid,j}$ $\frac{dm_{liquid,j}}{dt} = F_{feed,liquid} * w_{feed i,liquid} - F_{out,liquid} w_{liquid,j}$ <p>+ initial condition for $m_{solid,j}$ and $m_{liquid,j}$ (at time zero)</p> <p>With:</p> <p>ρ_{solid} = density solid phase, Kg/m³</p> <p>ρ_{liquid} = density liquid phase, Kg/m³</p> <p>V_{solid} = Volume solid phase, m³</p> <p>V_{liquid} = Volume liquid phase, m³</p> <p>$F_{feed,solid}$ = Solid Inlet stream mass flowrate, kg/s</p> <p>$F_{feed,liquid}$ = Liquid Inlet stream mass flowrate, kg/s</p> <p>$w_{feed i,solid}$ = weight fraction of component i in solid feed stream, Kg/Kg</p> <p>$w_{feed i,liquid}$ = weight fraction of component i in liquid feed stream, Kg/Kg</p> <p>Components and molecular weights need to be defined.</p> <p>Defined initial conditions are needed.</p>
Surge Farm (Two Vessel)		<ul style="list-style-type: none"> - Each vessel of the farm is treated as a well-mixed volume - Constant density - Multiple inputs, single output - Tanks are online one at a time and will switch when one tank is empty. - Total surge volume is initially distributed as defined by the user 	$\rho V_k = m_{t,k}$ $m_{j,k} = w_{j,k} m_{t,k}$ $F_{in} = \sum_{i=1}^N F_{feed,i}$ $F_{out} = F_{in}$ <p>When Farm_Status = "T1Online_T3Fill"</p>

		<p>between three vessels.</p> <ul style="list-style-type: none"> - At all times, one vessel is “online” (i.e. its contents define the outlet composition), another is “filling” while a third is full and “idle”. These switch instantaneously when a user specified heel amount is reached in the online vessel. - If not specified otherwise, vessel 2 always starts full with half of the initial total volume. 	$w_{j,out} = w_{j,1}$ $\frac{dm_{t,1}}{dt} = -F_{out}$ $\frac{dm_{j,1}}{dt} = -F_{out} w_{j,1}$ $\frac{dm_{t,2}}{dt} = 0$ $\frac{dm_{j,2}}{dt} = 0$ $\frac{dm_{t,3}}{dt} = \sum_{i=1}^{n_{feed}} F_{feed,i}$ $\frac{dm_{j,3}}{dt} = \sum_{i=1}^{n_{feed}} F_{feed,i} w_{feed\ i,j}$ <p>Switch to "T2Online_T1Fill" when $V_1 < V_t^o v_{heel}$ When Farm_Status = "T2Online_T1Fill"</p>
--	--	--	--

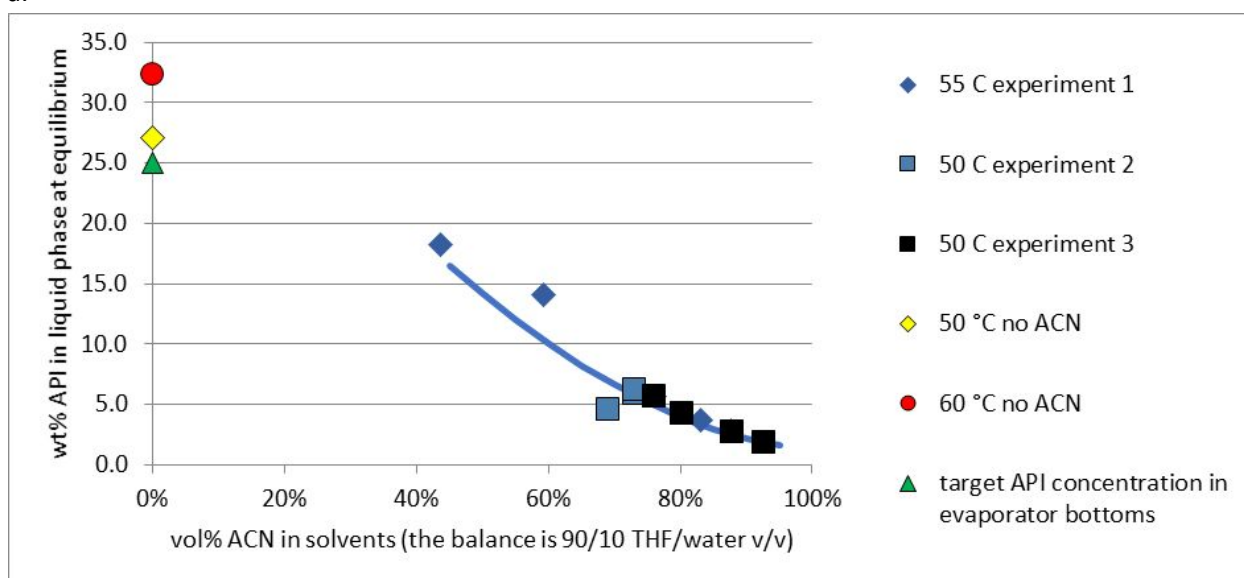
			$w_{j,out} = w_{j,2}$ $\frac{dm_{t,2}}{dt} = -F_{out}$ $\frac{dm_{j,2}}{dt} = -F_{out} w_{j,2}$ $\frac{dm_{t,1}}{dt} = \sum_{i=1}^{n_{feed}} F_{feed,i}$ $\frac{dm_{j,1}}{dt} = \sum_{i=1}^{n_{feed}} F_{feed,i} w_{feed\ i,j}$ $\frac{dm_{t,3}}{dt} = 0$ $\frac{dm_{j,3}}{dt} = 0$ <p>Switch to "T3Online_T2Fill" when $V_2 < V_t^o v_{heel}$ When Farm_Status = "T3Online_T2Fill"</p>
--	--	--	--

			$w_{j,out} = w_{j,3}$ $\frac{dm_{t,3}}{dt} = -F_{out}$ $\frac{dm_{j,3}}{dt} = -F_{out} w_{j,3}$ $\frac{dm_{t,2}}{dt} = \sum_{i=1}^{n_{feed}} F_{feed,i}$ $\frac{dm_{j,2}}{dt} = \sum_{i=1}^{n_{feed}} F_{feed,i} w_{feed\ i,j}$ $\frac{dm_{t,1}}{dt} = 0$ $\frac{dm_{j,1}}{dt} = 0$ <p>Switch to "T1Online_T3Fill" when $V_3 < V_t^o v_{heel}$</p> <p>With:</p> <p>ρ = density solution, Kg/m³</p> <p>V_t^o = Initial total volume, m³</p> <p>v_1^o = Initial volume fraction of half of the total volume in vessel 1 (One half is distributed between vessels 1 and 3, other half is in vessel 2. A value of 1 indicates vessel 1 has half of total)</p> <p>v_{heel} = Heel volume, expressed in fraction of initial total volume</p> <p>$w_{j,k}^o$ = Initial weight fraction of component j in vessel k, Kg/Kg</p> <p>$F_{feed,i}$ = Inlet stream i mass flowrate, kg/s</p> <p>$w_{feed\ i,j}$ = weight fraction of component j in inlet stream i, Kg/Kg</p> <p>Components and corresponding molecular weights need to be defined. Defined initial conditions are needed.</p>
--	--	--	---

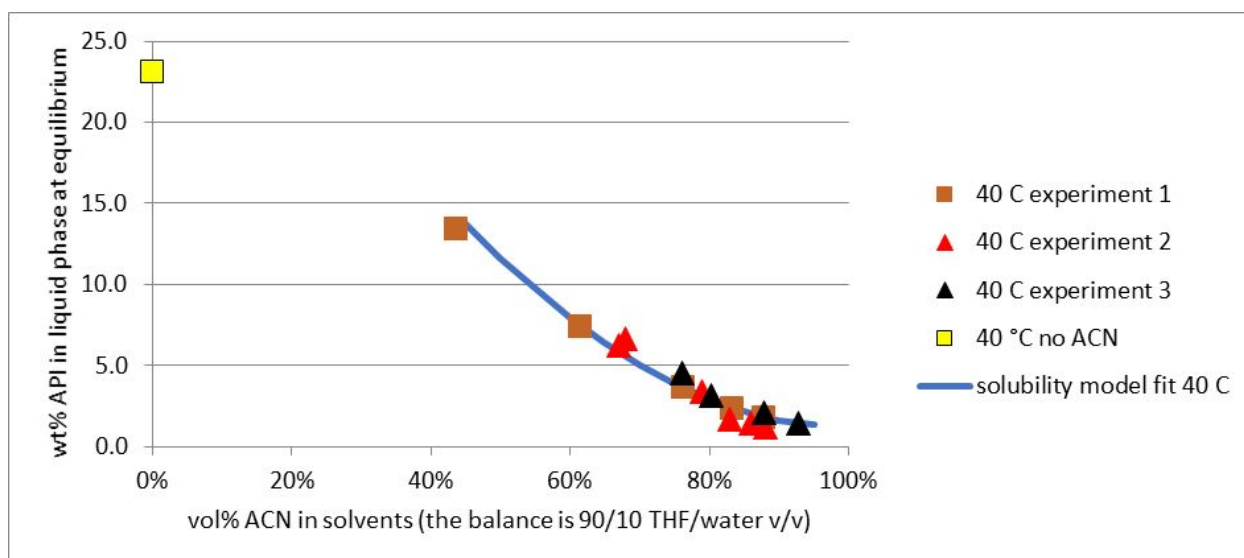
7. Solubility Measurements

API solubility data for 90/10 THF/water + ACN, as a function of temperature and volumes ACN, is given in Figure S16a-d. The figure also shows the solubility model fit to the data. In Figure S16d, the solids represented by the data point at 43% ACN, 10 °C, and 6.4 wt% solubility crystallized as the undesired monohydrate form, and the solids represented by the data point at 60% ACN, 10 °C, and 4.95 wt% solubility crystallized as a mixed anhydrate and monohydrate form. The anhydrate form was stable at all other conditions shown in the figures. Figure S16a shows a point for the distillation target concentration 25 wt% on the y-axis (0% ACN). This point represents the hot crude API solution entering MSMPR1 in the continuous process. For reference as it relates to the crude API feed entering MSMPR1, Figure S16a,b,c also show solubility data points on the y-axis for 0% ACN antisolvent, but these data points were not used for developing the solubility model.

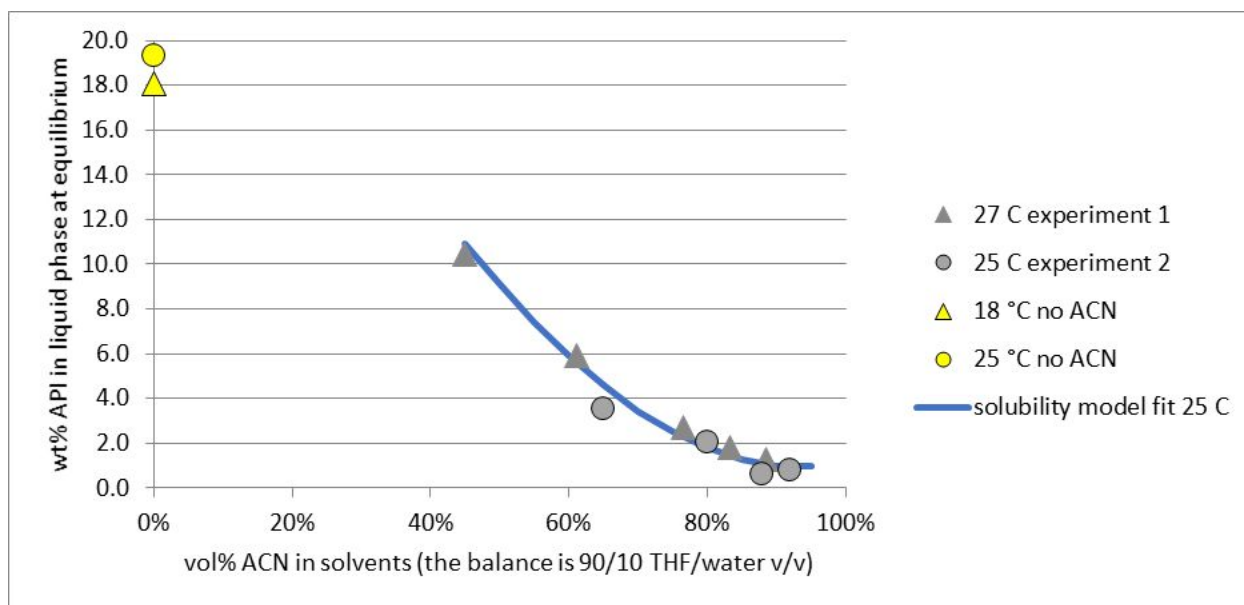
a.



b.



c.



d.

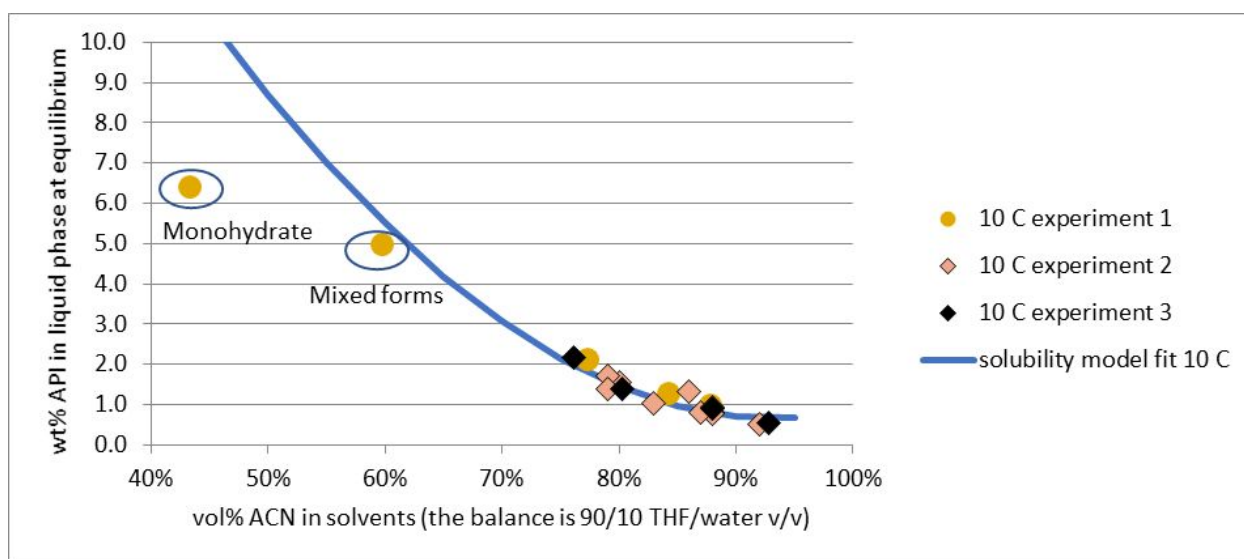


Figure S16. API solubility in 90/10 THF/water as a function of temperature and volumes ACN antisolvent added. (a) 50-60 °C (b) 40 °C (c) 18-27 °C (d) 10 °C

8. Population Balance Model – Scale Dependent

In this approach, growth and nucleation of crystals were assumed to follow power law kinetics. A relative supersaturation model, often cited in the literature⁷⁻⁹ was used for the growth rate expressions, G . A relative supersaturation power law-model was also used for secondary nucleation, J_{sec} . The major disadvantage of this approach is that the model is very scale dependent and does not allow for the

impact of mixing to be simulated as often times the specific power input ϵ and slurry density φ are not directly accounted in the model. Instead, the effects are buried in the secondary nucleation pre-factor. In this application, these effects were included in the secondary nucleation model. Effects of temperature on secondary nucleation were not included in this approach.

$$G = k_g \exp \left(- \frac{E_{A,g}}{RT} \right) \left[\frac{C_{bulk} - C_{sat}}{C_{sat}} \right]^g$$

$$J_{sec} = k_n \left[\frac{C_{bulk} - C_{sat}}{C_{sat}} \right]^n \epsilon^a \varphi^b$$

Where R is the gas law constant, and C is the concentration in the bulk (*bulk*), and of the saturated solution (*sat*). The other parameters are defined in Table S9.

Table S9: Population balance parameter value and variable descriptions for crystallization model 1.

Parameter	Description	Units	Value – research scale	Value – pilot scale	Value – Manufacturing scale
k_g	growth rate pre-factor	m/s	11	11	11
$E_{A,g}$	growth rate activation energy	J/mol	57754	57754	57754
G	growth rate order	-	2	2	2
k_n	secondary nucleation rate pre-factor	# m ⁻³ s ⁻¹	exp(15)	exp(14.25)	exp(13.6)
N	secondary nucleation rate order	-	1.5	1.5	1.5
A	energy dissipation rate order	-	0.5	0.13	0.29
B	slurry density order	-	0.57	0	0

Research Scale

Experiments R10, R11 and R15-R17 were used for obtaining parameter values and experiments R3-R9 were used to check model validity. The particle size distributions (quantiles x10, x50 and x90) measured at 30 h duration of continuous run were chosen. Initial model runs with approximate kinetics indicated that MSMPRs reached steady state after 20-25 h, hence 30 h duration data was used for parameter fitting. Also, the x90 quantile had more variance across experiments than either the x10 or x50. Accordingly, higher variance was assumed for the x90 value in the Maximum likelihood estimation. The following strategy was used for estimating the parameters in the kinetic rate expressions for growth and nucleation. Initial guesses for parameters k_g , k_b and $E_{A,g}$ were estimated by keeping other parameters constant ($g=2$, $n=2$, $a=1$, $b=1$). Then, using the estimated initial values, all the parameters were estimated simultaneously.

A parity plot of measured and predicted quantiles is shown in Figure S17. The model predicted x10 and x50 satisfactorily and under-estimated x90. Also, the variance in predicted values of x90 is more than x10 and x50 following the trend observed in predicted values. The model captured the experimental observation of particle size decrease in MSMPR3 compared to MSMPR2. Growth rate is highly sensitive to temperature due to the high activation energy and nucleation is likely to compete during low temperature conditions, which explains the observed decrease of particle size in MSMPR3 compared to MSMPR2 for the runs with a third MSMPR maintained at a low temperature.

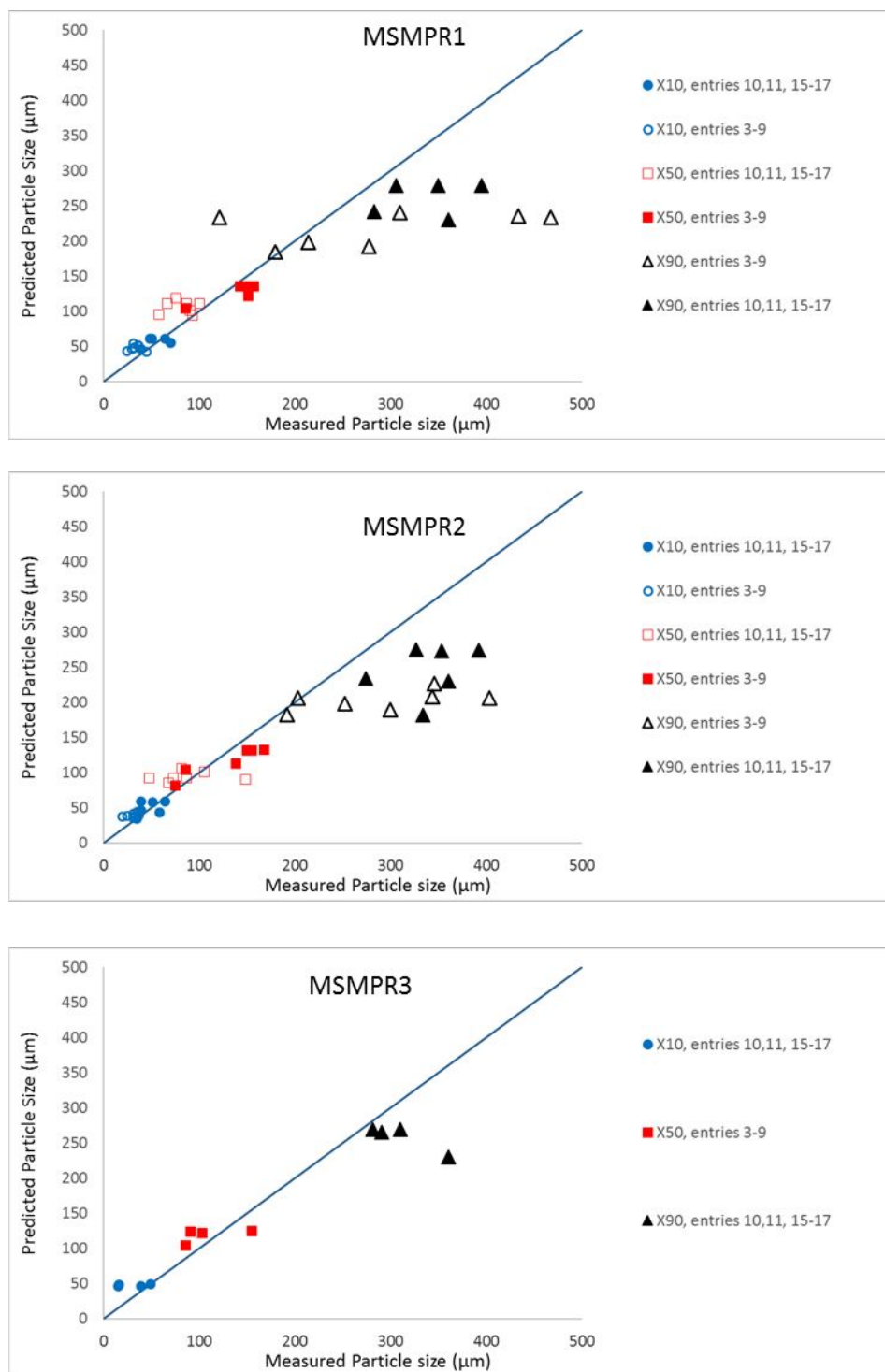


Figure S17. Parity plots of experimental and model predicted values of X10, X50, and X90 in MSMPR1, MSMPR2 and MSMPR3 using research scale experimental data. Filled symbols indicate entries used for estimation of parameter and open symbols indicate experiments used for validation of the model.

Pilot scale

The population balance model used for the research scale data was reparametrized using the pilot scale run data. Baseline conditions and the associated particle size distribution were used for refining nucleation rate parameters. The growth rate is expected to remain the same across research, pilot and manufacturing scales. Nucleation is expected to change with a change in hydrodynamics at different scales.^{10, 11} The power law expression used for the nucleation rate in the present work includes the energy dissipation term that should account for the impact of a change in scale due to a change in volume and agitation. However, application of the lab scale model to the pilot and manufacturing scale did not show parity. As a result, the nucleation rate parameters were re-estimated using the pilot experiment P4. Pilot scale experiment P3 was used for model validation.

Re-estimated nucleation parameters are shown in Table S9, for comparison to research and manufacturing scales. The calculated nucleation rate is lower at pilot scale and manufacturing scale compared to the research scale. Figure S18 shows a parity plot of measured and predicted particle size quantiles. As observed with the research scale predictions, the x10 and x50 were predicted well while the x90 was under predicted. The high value of x90 could be the result of non-uniform suspension of solids, and consequently a higher residence time than the liquid residence time.

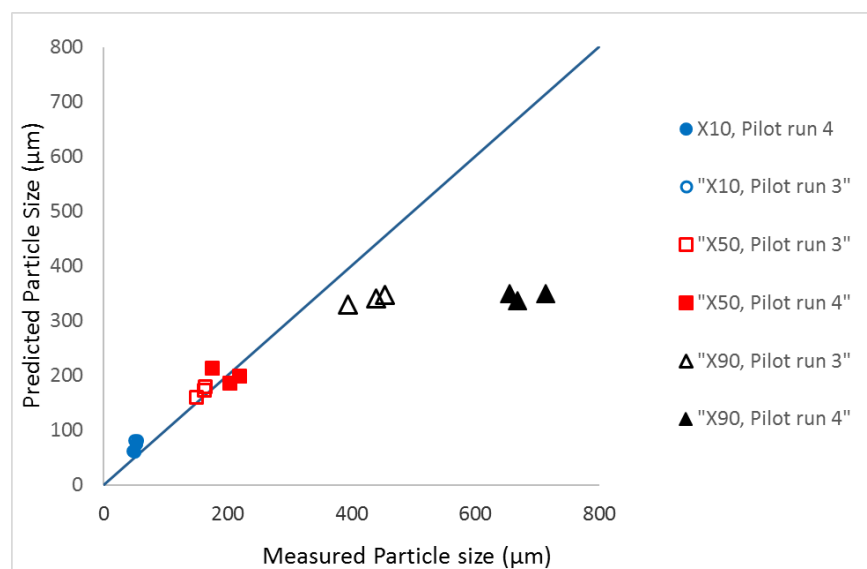


Figure S18. Parity plot of experimental and model predicted values of X10, X50, and X90 using pilot scale run data. Filled symbols indicate entries used for estimation of parameter and open symbols indicate experiments used for validation.

Manufacturing scale

Population balance modeling was also performed to simulate the manufacturing conditions, modifying the model described previously to account for the change in scale. Table S10 shows the model predicted particle size for the base conditions of the manufacturing run. Comparing the predictions with the average of the observed values indicates that the model captures the x10 and x50 better than x90. The average values for x10, x50, and x90 for the 18 manufacturing batches were 68, 271, and 580 μm,

respectively. In manufacturing, no samples were taken from MSMPR1 and MSMPR2 for particle size analysis.

Table S10. Model predictions of particle size after 30 h for base case conditions at manufacturing scale

MSMPR	x10 (μm)	x50 (μm)	x90 (μm)
1	88	197	390
2	83	191	386
3	78	190	378
3 – Ave. Expt Data	68	271	580

9. References

1. Albert, F.; Augustin, W.; Scholl, S., Roughness and constriction effects on heat transfer in crystallization fouling. *Chemical Engineering Science* **2011**, *66*, 499-509.
2. Vendel, M.; Rasmuson, Å. C., Initiation of Incrustation by Crystal Collision. *Chemical Engineering Research and Design* **2000**, *78*, 749-755.
3. Marangoni, C., Ueber die Ausbreitung der Tropfen einer Flüssigkeit auf der Oberfläche einer anderen. *Annalen der Physik* **1871**, *219*, 337-354.
4. Scriven, L. E.; Sternling, C. V., The Marangoni Effects. *Nature* **1960**, *187*, 186-188.
5. The R Core Team *R: A Language and Environment for Statistical Computing*, R Foundation for Statistical Computing: Vienna, Austria, 2020.
6. Wickham, H., *ggplot2: Elegant Graphics for Data Analysis*. Springer-Verlag: New York, 2016.
7. Zipp, G. L.; Rodriguez-Hornedo, N., Determination of crystal growth kinetics from desupersaturation measurements. *International Journal of Pharmaceutics* **1989**, *51*, 147-156.
8. Kougoulos, E.; Jones, A. G.; Wood-Kaczmar, M. W., Estimation of crystallization kinetics for an organic fine chemical using a modified continuous cooling mixed suspension mixed product removal (MSMPR) crystallizer. *Journal of Crystal Growth* **2005**, *273*, 520-528.
9. Mangood, A.; Malkaj, P.; Dalas, E., Hydroxyapatite crystallization in the presence of acetaminophen. *Journal of Crystal Growth* **2006**, *290*, 565-570.
10. Steendam, R. R. E.; Keshavarz, L.; Blijlevens, M. A. R.; de Souza, B.; Croker, D. M.; Frawley, P. J., Effects of Scale-Up on the Mechanism and Kinetics of Crystal Nucleation. *Crystal Growth & Design* **2018**, *18*, 5547-5555.
11. Tung, H. H.; Paul, E. L.; Midler, M.; McCauley, J. A., *Crystallization of Organic Compounds: An Industrial Perspective*. Wiley Books 2009.